Advances in Nano Research, *Vol. 10, No. 2 (2021) 191-210*
DOI: https://doi.org/10.12989/anr.2020.10.2.191

Effect of method of synthesis on antifungal ability of ZnO nanoparticles: Chemical route vs green route

Melissa C. Patiño-Portela[1], Paola A. Arciniegas-Grijalba[1], Lyda P. Mosquera-Sánchez[1], Beatriz E. Guerra Sierra[2], Jaime E. Muñoz-Florez[3], Luis A. Erazo-Castillo[4] and Jorge E. Rodríguez-Páez*[4]

[1]*Grupo de Investigación en Microscopia y Análisis de Imágenes (GIMAI), Universidad del Cauca, Popayán, Colombia*
[2]*Grupo de Investigación en Biotecnología Agroambiente y Salud-Microbiota, Universidad de Santander, Bucaramanga, Colombia*
[3]*Grupo de Investigación en Diversidad Biológica, Universidad Nacional de Colombia, Sede Palmira, Colombia*
[4]*Grupo de Investigación en Ciencia y Tecnología de Materiales Cerámicos (CYTEMAC)*
Departamento de Física, Universidad del Cauca, Popayán, Colombia

(*Received February 13, 2020, Revised October 26, 2020, Accepted January 6, 2021*)

Abstract. To compare the antifungal effect of two nanomaterials (NMs), nanoparticles of zinc oxide were synthesized by a chemical route and zinc oxide-based nanobiohybrids were obtained using green synthesis in an extract of garlic (*Allium sativum*). The techniques of X-Ray Diffraction (XRD), Infrared (IR) and Ultraviolet Visible (UV-Vis) absorption spectroscopies and Scanning (SEM) and Transmission Electron Microscopies (TEM) were used to determine the characteristics of the nanomaterials synthesized. The results showed that the samples obtained were of nanometric size (< 100 nm). To compare their antifungal capacity, their effect on *Cercospora* sp. was evaluated. Test results showed that both nanomaterials had an antifungal capacity. The nanobiohybrids (green route) gave an inhibition of fungal growth of ~72.4% while with the ZnO-NPs (chemical route), inhibition was ~87.1%. Microstructural studies using High Resolution Optical Microscopy (HROM) and ultra-structural analysis using TEM carried out on the treated strains demonstrated the effect of the nanofungicides on the vegetative and reproductive structures, as well as on their cell wall. To account for the antifungal effect presented by ZnO-NPs and ZnO nanobiohybrids on the fungi tested, effects reported in the literature related to the action of nanomaterials on biological entities were considered. Specifically, we discuss the electrical interaction of the ZnO-NPs with the cell membrane and the biomolecules (proteins) present in the fungi, taking into account the n-type nature of the ZnO semiconductor and the electrical behavior of the fungal cell membrane and that of the proteins that make up the protein crown.

Keywords: ZnO nanofungicides; green synthesis; chemical synthesis; antifungal capacity; phenomenological model

1. Introduction

Nanostructured materials (NSs) and nanoparticles (NPs) have unique or enhanced properties in relation to their macro-scale counterparts (Heiligtag and Niederberger 2013, Khan *et al*. 2017). This occurs because surface effects and quantum effects begin to be more evident on reducing the size of the particles (Buzea *et al*. 2007, Nealon *et al*. 2012). The unique properties of NPs involve the increase in their reactivity and adsortivity due to their high specific surface. When particle size decreases below 100 nm, the ratio of surface area to volume decreases dramatically, a condition that leads to the nanoscale materials or nanomaterials (NMs) having a large proportion of their atoms exposed superficially, giving a different disposition of atomic sites compared to their bulk material counterpart (Klingshirn 2007). The surface of the nanosized colloids would mainly be constituted of under-coordinated atoms that would favor the localization of specific defects.

Moreover, when the surface-to-volume ratio is large, there is a greater population of edge and corner sites that are considered the most reactive, since these are the sites with the highest coordination (Lear *et al*. 2005). This condition justifies the high surface energy and reactivity of the NPs (Cui *et al*. 2016). Currently, these unique or amplified properties of NPs have aroused great scientific and technological interest, specifically in the field of environmental nanotechnology (Xing *et al*. 2016). Due to the high chemical reactivity, surface adsorption ability and surface charge presented by NPs, they interact efficiently with biological systems, causing significant toxicity (Fiévet and Brayner 2013, Nel *et al*. 2006, Ray *et al*. 2009). This behavior has led to considering their use in the control of phytopathogenic fungi (Prasad 2016, Tripathi *et al*. 2017) such as nanofungicides (Abd-Elsalam and Alghuthaymi 2015), as is the case with the biohybrid nanocide materials that are being used as a new environment-friendly antimicrobial against different pathogenic fungal organisms of plants (Abd-Elsalam and Alghuthaymi, 2015).

Nanoparticles - and nanofungicides in particular - have in the main been synthesized by physicochemical processes that do not have a high efficiency, as occurs in the synthesis of chemical products in general (Trost 1991). This low

*Corresponding author, Ph.D.,
E-mail: jnpaez@unicauca.edu.co

ISSN: 2287-237X (Print), 2287-2388 (Online)

efficiency of synthesis processes, especially organic in nature, generates great concern for the management of chemical waste and the challenges related to conservation of resources. These processes cause environmental pollution (Mitchnick *et al*. 1999), which has led to considering the development of greener processes (Li 2016, Virkutyte and Varma 2013). Since chemical reactions play a fundamental role in the synthesis of products, including NPs, "Green chemistry" is developing processes ("green synthesis") that involve chemical reaction conditions that provide benefits related to resources and energy efficiency, product selectivity, operational simplicity and both sanitary and environmental safety, among others. For this, innovative reactions with inherent advantages have been evaluated and considered, seeking, for example, a direct conversion of C-H links into desired structures without the need for additional chemical transformations (Arndtsen *et al*. 1995, Crabtree 2004). In nature this process occurs frequently, since a variety of organic compounds can easily be oxidized by molecular oxygen or other oxygen donors in the cells of bacteria, fungi, plants, insects, fish and mammals (Shapiro and Caspi 1998). Another innovative aspect, also related to chemical reactions, is synthesis without protection. The nature of classical chemical reactivity of reactions that occur during the synthesis of products, such as nanoparticles, involves stages of protection-deprotection of functional groups, increasing the number of steps in obtaining the desired compound. It is necessary therefore to favor synthesis processes without protection and de-protection (Li 2016, Li and Trost 2008).

Undoubtedly, an important innovation in the NP synthesis process would be related to the type of solvent used (Sheldon 2005). The solvent is an auxiliary material employed during synthesis and although not an integral part of the compound undergoing the reaction, it plays an important role in the chemical production of the product of interest. In classical chemical processes, the solvent is used to dissolve reagents, extract and wash products, separate mixtures and disperse products for practical applications. In classical chemical synthesis, the solvent should further facilitate mass transfer in order to modulate chemical reactions in terms of reaction rate, efficiency, conversion and selectivity (Li and Trost 2008). The ironic aspect of the process is that, after the reaction occurs, the final product must be separated from the solvent, requiring energy-costly methods. Green synthesis re-defines the role of the solvent, considering that it should facilitate mass transfer, but not dissolve. The green solvent should ideally be natural, non-toxic, cheap and easily available. Considering these requirements, the most suitable solvents would be water (Narayan *et al*. 2005) and CO_2 (Beckman 2003). In the current study, water was used to obtain ZnO nanofungicides by green synthesis, because it is a cheap, natural, environmentally friendly solvent. In addition, hydrophobic effects that can occur with its use during the process could not only accelerate the reaction rates but increase the selectivity of the reaction, even if the reagents were partially soluble or insoluble in the medium (Li and Trost 2008, Rideout and Breslow 1980). Furthermore, using water as a solvent could eliminate the tedious process of protection-deprotection for certain acidic, hydrogen-containing functional groups, an action that would contribute to the overall efficiency of the process.

Specifically, research is currently being carried out related to the synthesis of NPs of zero-valent metals, metal oxides, and salts, using greener routes (Kharissova *et al*. 2013), given the importance of developing technologies for the future, for humanity and the environment (Parveen *et al*. 2016). Green synthesis emerges as an alternative to reduce the use of dangerous compounds and harsh reaction conditions in the production of NPs. As such, if NP synthesis were carried out using environmentally friendly and biocompatible reagents, the toxicity of the obtained material could be favorably affected and the environmental impact of the byproducts reduced (Li and Trost 2008).

The Zinc Oxide Nanoparticles (ZnO-NPs) of interest for this work and that are used in a large number of technological applications (Jagadish and Pearton 2006, Klingshirn 2007, Klingshirn *et al*. 2010, Morkoç and Özgür 2008) for their optical properties (Djurišić and Leung 2006), their semiconductor nature (Janotti and Van de Walle 2009) and for the physicochemical properties of their surface (Woll 2007) have been used in environmental remediation (Kisch 2014, Lead and Smith 2009, Sheldon 2005), specifically as antifungals (Arciniegas-Grijalba *et al*. 2017, Kairyte *et al*. 2013, He *et al*. 2011, López and Rodríguez-Páez 2017, Sharma *et al*. 2010), with high effectiveness. They have been synthesized using different methods (Kołodziejczak-Radzimska and Jesionowski 2014). Several stand out, including precipitation (Moharram *et al*. 2014, Rodríguez-Paéz *et al*. 2001), Pechini polymerizable complex (Avila *et al*. 2004), combustion (Guo and Peng 2015), sol-gel (Alwan *et al*. 2015), hydrothermal (Yang *et al*. 2015) and polyol process (Dakhlaoui *et al*. 2009). ZnO-NPs have also been obtained through green synthesis (Agarwal *et al*. 2017, Ahmed *et al*. 2017, Hussain *et al*. 2016) and biological methods using, for example, extracts of flowers (Ambika and Sundrarajan 2015, Dobrucka and Długaszewska 2016), fruits (Jafarirad *et al*. 2016), fruit peel (Jayaram *et al*. 2017), freeze-dried leaf peel (Qian *et al*. 2015), coconut milk (Krupa and Vimala 2016) and leaves and cellulosic fiber (Aladpoosh and Montazer 2015, Ali *et al*. 2016, Anbuvannan *et al*. 2015). The ZnO obtained by green synthesis was found, on several occasions, to have a greater antibacterial effect than the chemically synthesized one (Dobrucka and Długaszewska 2016), appreciably affecting multi-drug resistant clinical bacteria (Ali *et al*. 2016).

In this work, ZnO-NPs were synthesized by a chemical route, while ZnO-based nanobiohybrids were obtained using green synthesis, in order to determine the antifungal capacity of each on the *Cercospora* sp. fungus, a pathogen of the coffee crop. To synthesize the nanobiohybrids, an extract of garlic (*Allium sativum*) was used as synthesis solvent, since multiple biological activities are attributed to garlic (Ledezma and Apitz-Castro 2006), including its anti-fungal capacity (Aala *et al*. 2014, Muhsin *et al*. 2001, Tansey and Appleton 1975, Timonin and Thexton 1951, Yoshida *et al*. 1987). Antifungal evaluation showed that the efficiency of the nanofungicides depended as much on the

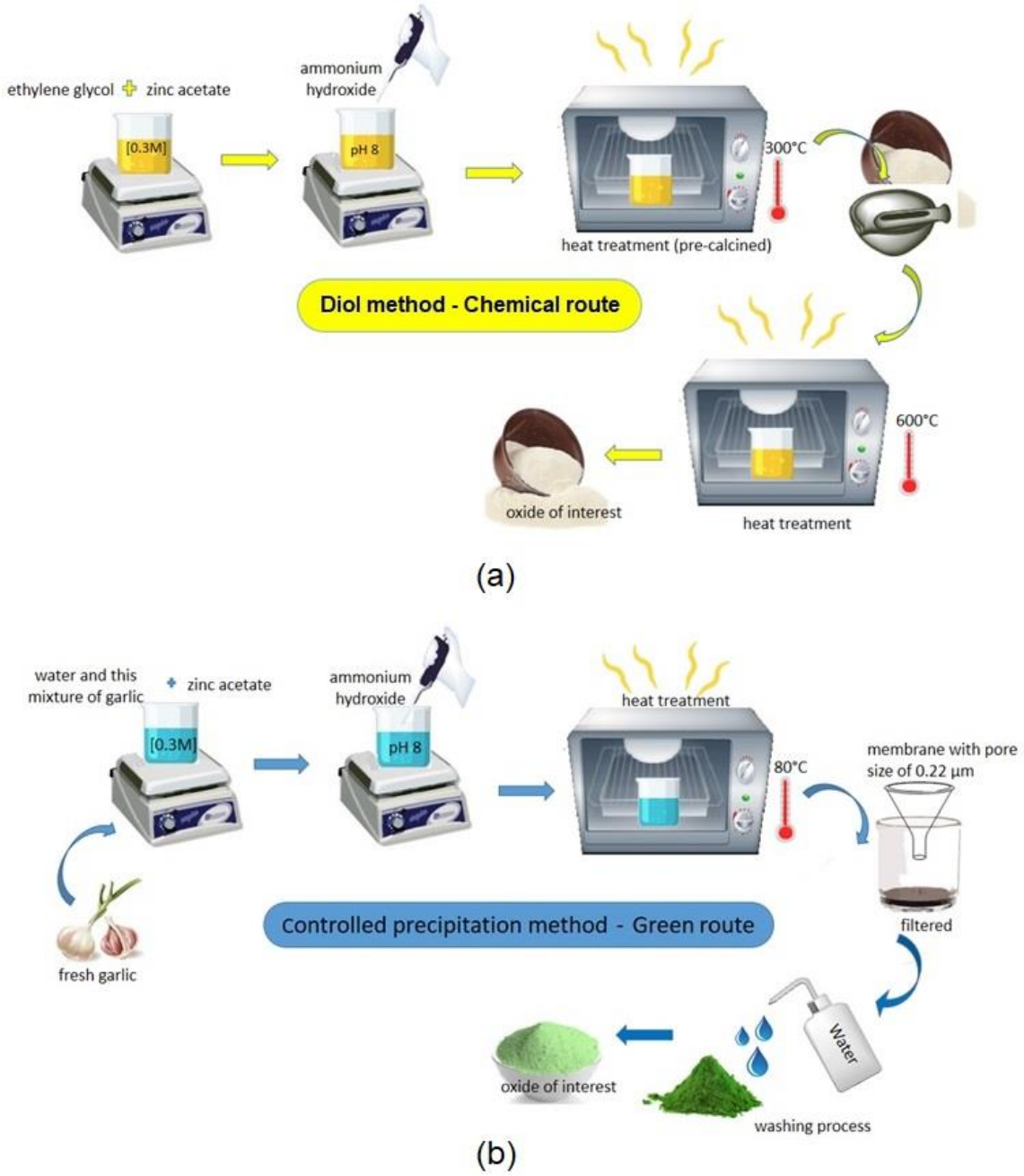

Fig. 1 Synthesis processes used to obtain ZnO-based nanomaterials by a (a) chemical route and by (b) green synthesis

technique of obtaining them, i.e., chemical or green synthesis, as on fungal characteristics such as evolutionary adaptations and the expression of a number of fungal genes involved both in the uptake of ZnO and in the response to oxidative stress, an aspect reported recently (Li *et al*. 2017).

2. Materials and methods

2.1 Obtaining ZnO-NPs by a chemical route

The ZnO nanomaterials (ZnO-NMs) used in this work were synthesized using the methodology described in a previous paper (Arciniegas-Grijalba *et al*. 2019). To obtain the ZnO-NPs using a chemical route, a certain amount of zinc acetate ($Zn(O_2CCH_3)_2(H_2O)_2$ - AcZn Merck) was taken and dissolved in ethylene glycol ($C_2H_6O_2$ - Merck) (Fig. 1(a)). The mixture was stirred until the solution became completely transparent. The resulting solution was acidified with nitric acid (HNO_3 - Merck) until reaching a pH of 4. Ammonium hydroxide ((NH_4OH) - Merck) was added to this mixture at a rate of 1 mL/min, making use of the Metrohm 775 Dosimat, maintaining the mixture in continuous agitation until reaching pH 8. Distilled water was then added to the system to promote hydrolysis reactions within it. NH_4OH was again added to the solution until reaching a pH of 9.5. To remove the solvent, the obtained suspension was dried on a hotplate for 6 hours at 150°C. The resin obtained, viscous in nature, was subjected to heat treatment at 300°C, obtaining a brown solid (pre-

calcined material). This solid was macerated in an agate mortar until obtaining a very fine powder, a material that was subjected to a heat treatment at 600°C for 4 hours using a Thermolyne furnace, obtaining the ZnO of interest.

2.2 Obtaining ZnO-based biohybrid nanomaterials by means of green synthesis

To synthesize the ZnO nanobiohybrid by a green route, a plant was used that reports antifungal capacity, namely garlic (*Allium sativum*). For this, samples of garlic were obtained in a popular store. These were taken to the microbiology laboratory where the husk was removed and weighed. Next, 10 g of fresh, washed and disinfected fresh garlic was added to 100 mL of water and this mixture was blended at room temperature using an Oster 6381 blender. The product obtained was filtered and the filtrate stored at 4°C for subsequent use. The ZnO nanobiohybrid was synthesized by controlled precipitation (Fig. 1(b)). For this, zinc acetate dihydrate ($Zn(O_2CCH_3)_2(H_2O)_2$ - AcZn) was also used as the zinc precursor, and the garlic extract in distilled water as a solvent. The obtained suspension was stirred at room temperature and acidified with nitric acid (HNO_3) until obtaining a pH of 4 in the system. The NH_4OH was then added to the suspension at a rate of 2 mL/min under continuous agitation of the system (200 rpm), and the increase in the pH of the system was carried out in a controlled manner until reaching a pH of 8.5. The process was carried out at room temperature and the resulting precipitate was allowed to age for 1 day.

After this time, the obtained suspension was filtered using a membrane with pore size of 0.22 μm and the solid obtained was dried and re-dispersed in a volume of garlic extract similar to that used during synthesis, using a high shear disperser (IKA-T50), at 10.000 rpm, for 20 minutes. This process of re-dispersion, aging and filtration of the precipitate was repeated five times every 24 hours and after each stage a solid sample was taken, which was characterized with IR spectroscopy to determine the evolution of the functional groups present in it. This stage was implemented in the synthesis process in order to favor the direct conversion of the C-H bonds into desired structures and to avoid the heat treatment that would favor the chemical transformation to ZnO, as occurred in the chemical synthesis. The resulting product, after carrying out the washing process, was dried in a furnace at 80°C, for 12 hours, and macerated in an agate mortar. The solid obtained in each washing step was characterized to determine the evolution of the solid phase during the synthesis process.

2.3 Characterization of the synthesized nanomaterials

The samples obtained through the synthesis processes described above were characterized using various conventional techniques. IR spectroscopy was used to determine the different functional groups present in the samples of interest. The sample to be analyzed was obtained by mixing dry KBr with the synthesized solid. The scan was carried out between 4000 cm^{-1} and 400 cm^{-1} using a Thermo Nicolet IR 200 spectrophotometer.

To determine the possible electronic transitions that may occur in the solid of interest, UV-Vis absorption spectroscopy was used, using the Thermo Spectronic Genesys equipment. The synthesized samples were dispersed in distilled water, in concentrations of 0.1 and 0.2 g/mL, and the suspension was emptied into 1 cm high quartz cells that were placed in the chamber of the equipment for analysis. The scan was performed between 190 and 750 nm.

To determine the crystalline phases present in the samples synthesized, X-ray diffraction was used. XRD patterns of the solids of interest, in powder, were obtained using a Bruker D8 Advance X-ray diffractometer, using $K\alpha$ radiation from Cu (λ = 1.542 Å) in the range of 10 to 70 in 2θ.

The size and morphology of the particles, as well as their state of agglomeration, were determined using electron microscopy. To obtain the micrographs in Transmission Electron Microscopy (TEM), the synthesized solids were suspended in 1 mL of ethanol and this suspension was placed in an ultrasonic bath, for one hour. Subsequently, using a Pasteur pipette, a small amount was taken and deposited on a nickel grid previously covered with a Formvar membrane. The grid was placed in the sample holder of a Jeol JEM 1200 EX electron microscope and the sample was observed.

Meanwhile, in order to obtain micrographs with Scanning Electron Microscopy (SEM), the FE SEM JSM-7100F equipment was used. To this end, a double-sided carbon tape was used, on which the solid to be analyzed was dispersed. This disposition of the sample was placed in the sample of the equipment and its analysis proceeded with.

2.4 Methodology used to determine the action of nanomaterials on coffee pathogens

To determine the percentage inhibition of ZnO-based nanofungicides on coffee pathogen strains, a three-part method was developed. For this, an experimental design was proposed in randomized complete blocks (days), in triplicate, for which the action of the treatments over time was considered, depending on the growth of each fungus. Initially, solid mycological culture media (potato dextrose agar) were prepared to form on them a culture medium without any treatment (control) and a second culture medium containing ciproconazole (120 μL) (a fungicide), as well as three treatments that contained the culture medium and the ZnO-NPs in concentrations of 6 $mmol.L^{-1}$ (T1), 9 $mmol.L^{-1}$ (T2) and 12 $mmol.L^{-1}$ (T3).

To obtain homogeneity and reproducibility in planting, a 16-day-old fungus was used to guarantee the existence of growth structures, employing a 1.5 cm diameter punch as the standard size of fungal inoculums. These were deposited in the center of each box of culture medium, for each of the nanofungicide treatments considered. ZnO-NPs and ZnO nano-biohybrids (obtained by means of the method developed by Arciniegas-Grijalba *et al*. (2019)) were incorporated into prepared media taking account of the

indicated experimental design.

Monitoring of the culture media was started from the third day after sowing and a photographic record of the crops was taken periodically, until the control completely covered the petri dish (for example, for *Cercospora* sp., 12 days). These records were then taken to the "Image pro Analyzer" image analysis system to measure the growth area or the inhibition halo.

Finally, using the data from the periodic recording of growth area (measured in cm^2), statistical analysis was performed to determine if the differences observed in this parameter were statistically significant. All data were subjected to a normal curve adjustment and homogeneity of variance analysis, and on meeting these two criteria, the two-way ANOVA test was used, using the BioStat 5.3 program (Zar 2014). The graphics were constructed using the GraphPad program (Motulsky 2007), obtaining the bar diagrams that visually revealed the most efficient treatment in terms of inhibition.

To obtain quantitative information on the efficiency of these treatments, with the same data used to obtain the bar charts, percentage inhibition was determined using the following equation

$$\% \text{ inhibition} = \frac{\text{Growth of control} - \text{Growth of treatment}}{\text{Growth of control}} \times 100 \quad (1)$$

2.5 Identification of morphological and ultra-structural damage in the fungi

2.5.1 Preparation of the samples

The samples of the fungal isolates used for the ultra-structural analysis were previously selected considering the inhibitory effect produced by the action of the nanofungicides. These were processed according to the standard protocol for transmission electron microscopy (Romero de Pérez 2003). Small samples of the selected isolates were placed in Eppendorf vials. They were then fixed overnight in a 2.5% glutaraldehyde mixture at 4°C. The following day the fixative was removed and the samples were washed three times with phosphate buffer (PBS), for five minutes each time. They were then post-fixed with osmium tetra-oxide (OsO_4) at 1%, for 1 hour at room temperature, and then washed again with buffer, three times for five minutes each time. The post-fixed samples were dehydrated with ethanol in ascending concentrations of 30%, 50%, 70%, 80%, 90%, 95% and 100%, with a holding time of 10 minutes in each alcohol concentration. The pre-imbibition was carried out using a mixture of alcohol and LR White resin in proportions of 3:1, 1:1, 1:3, for 45 minutes for the first two proportions, and the other was left for 1 hour.

Finally, the samples were placed in gelatin capsules, labeled and included in LR White resin, polymerized in an ultraviolet chamber at room temperature for 48 hours. Once the samples were polymerized, the capsules were taken and scraped with a double-edged knife so as to eliminate the excess resin and be able to obtain semi-fine sections of 200-300 nm and ultra-fine sections of 40-60 nm. The semi-fine and ultra-fine sections were obtained using a glass blade with the aid of an ultramicrotome (Leica Ultracut R).

2.5.2 High resolution optical microscopy (HROM)

• Imprint: Using transparent tape, samples were taken directly from the culture media, taking into consideration the control treatment and the treatment with nanofungicide, taking into account the concentration that had the greatest inhibitory effect on the growth of the strain. Subsequently, the imprint was placed on a slide, with a drop of lactophenol blue, and underwent observation using the Nikon Microphot MOAR. Images of interest were recorded using a Nikon Digital Sight DS-2Mv camera linked to the microscope, using the "Nis Elements" program for image capture.

• Analysis of semifine sections: The semifine sections cuts, 200-300 nm thick, were fixed with heat on the glass slide plates, stained with toluidine blue, flaming the plate and washing with distilled water. These sections were observed in the light field microscope (Nikon Microphot) using 40x and 100x lenses in order to select the area of greatest interest where the greatest number of hyphal structures were found, arranged transversely and longitudinally. This area was delimited and detailed again to obtain the ultra-fine sections.

2.5.3 Transmission electron microscopy (TEM)

Analysis and the ultra-structural description, looking at the effect of the nanofungicides on the selected isolates, was carried out by observing the TEM micrographs taken at different magnifications with the Jeol JEM 1200 EX operated at 80 Kv (Bozzola and Russell 1999).

• Contrast with uranyl acetate-lead citrate: The ultrafine cuts of 40-60 nm (ranging from gray to silver in color) were collected on copper grids coated with formvar membranes. These were contrasted with 4% uranyl acetate, for 20 minutes, using the humid, dark chamber flotation method. They were washed by dripping distilled water and then placed in contact with a drop of lead citrate, for 10 minutes, in a humid chamber containing tablets of sodium hydroxide (NaOH). Finally, the sections were washed with distilled water, dried with filter paper and observed in TEM (Bozzola and Russell 1999).

3. Results

3.1 IR spectra corresponding to synthesized nanomaterials

In the spectrum of Fig. 2(a) corresponding to the ZnO solid obtained by a chemical route, a band appears at 3435 cm^{-1} that can be associated with the hydroxyl groups, as does an intense band close to 450 cm^{-1}, characteristic of zinc oxide. The small bands located between 730 and 1500 cm^{-1} can be associated with the presence of superficially absorbed species (for example groups containing carbon) and the presence of structural defects where H^+ and H^- species would be found due to the presence of impurities from hydrogen within oxygen vacancies, as occurs in other

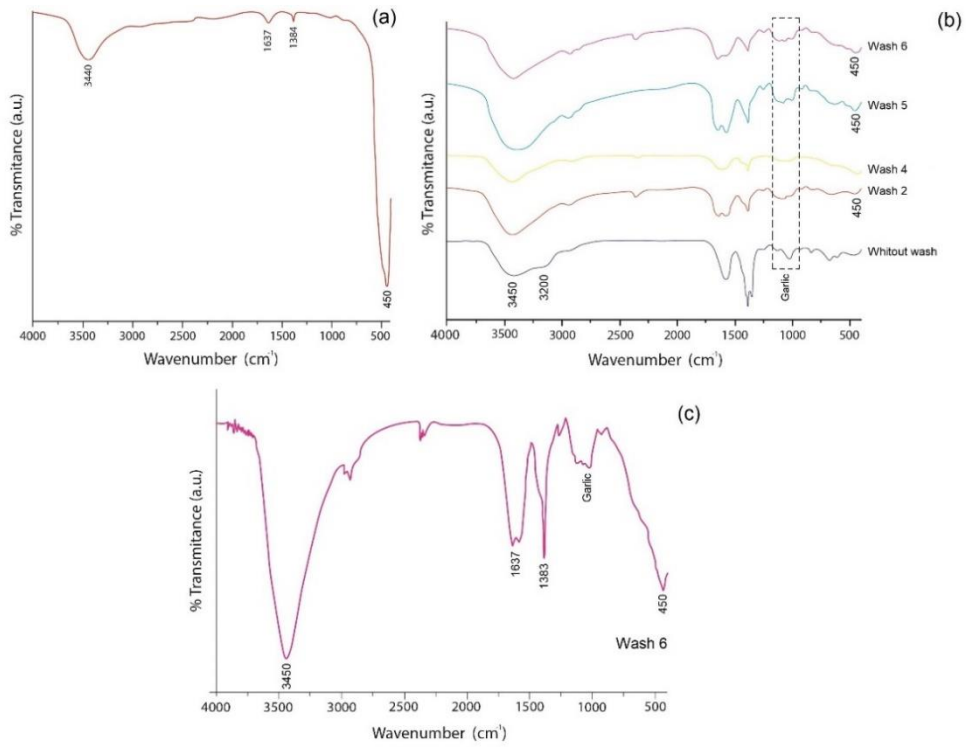

Fig. 2 (a) IR spectrum corresponding to a synthesized solid sample, heat treated at 600°C; (b) IR spectra of solid samples obtained in different stages of the process of washing with a water + garlic solution, during the green synthesis of the nanohybrid and, specifically, that corresponding to the solid of the (c) sixth wash

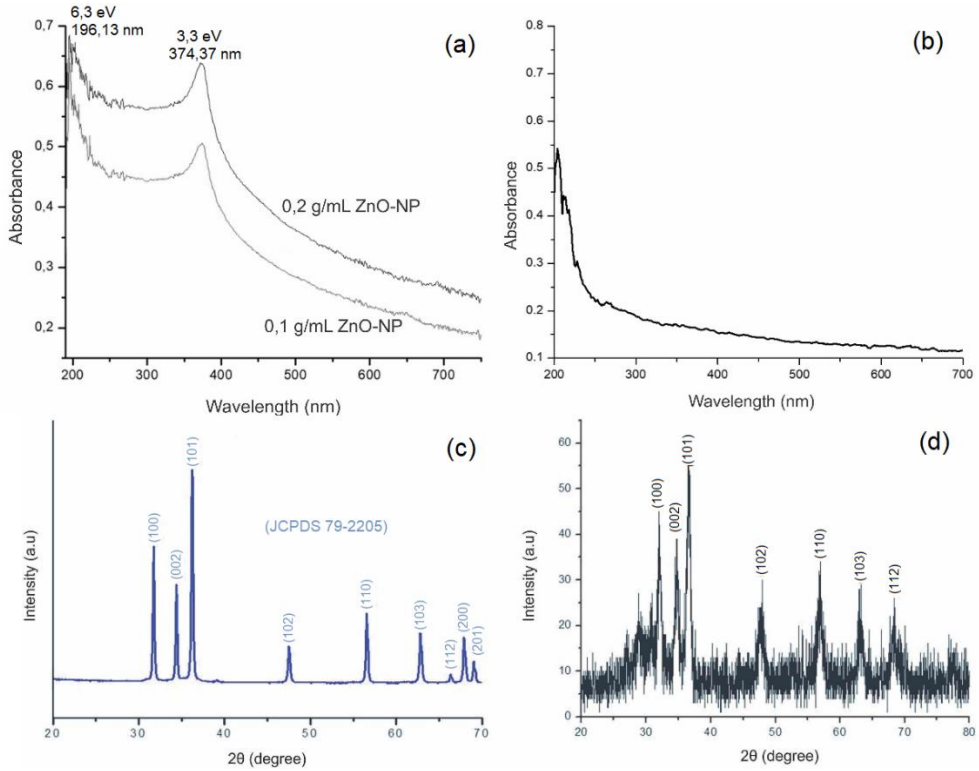

Fig. 3 UV-Vis absorption spectra and X-ray diffractograms corresponding to samples synthesized by chemical route ((a) and (c)) and green route ((b) and (d))

systems (Kumar and Kumar 2008a, b, Stankic *et al*. 2010).

In the IR spectrum corresponding to the unwashed nanohybrid sample (Fig. 2(b)), the bands characteristic of NH_3 (3200 cm^{-1}), hydroxyl (around 3500 cm^{-1}), COO^-

(doublet around 1500 cm^{-1}), and garlic (band around 1000 cm^{-1}) are observed. As the washing process progressed, on using the water + garlic solution (Fig. 2(b)) the bands associated with the CH bonds and the NH_3 and COO^- functional groups were significantly reduced, the bands associated with garlic (~1000 cm^{-1}) and that characteristic of ZnO (~450 cm^{-1}) being more evident (Figs. 2(b) and (c)). This result indicates that employing the washing process achieved a direct conversion of CH bonds to desired structures (wurtzite type ZnO) (Fig. 2(b)), one of the innovative aspects of interest for green chemistry. Specifically, for the solid obtained from the sixth wash with the water + garlic solution, Fig. 2(c), its IR spectrum clearly showed the band characteristic of ZnO, around 450 cm^{-1}. Bands were also observed, between 1550 and 1000 cm^{-1}, that can be associated to organic functional groups, whose origin would be primarily the garlic used during the synthesis process, although the contribution of the COO^- group from the precursor cannot be ruled out.

3.2 UV-Vis absorption spectra for the synthesized samples

The UV-Vis absorption spectrum of ZnO synthesized by a chemical route is shown in Fig. 3(a). It shows a band at 370 nm that can be associated with a valence band-conduction band electron transition, related to the width of the band energy (energy gap) and whose value would be ~3.3 eV. In addition, transitions are observed in the visible (> 400 nm) where the structural defects present in the sample would intervene. The bands located between 200 and 350 nm would correspond to electronic transitions between orbitals located on the Zn^{2+} and O^{2-} ions (charge exchange), evidencing quantum confinement effects. In Fig. 3(b), the UV-Vis absorption spectrum corresponding to a nanobiohybrid is synthesized by the green route, using water + garlic as solvent (sixth wash). In this spectrum, the absorption band corresponding to the inter-band electronic transition characteristic of ZnO is not observed. Only a band between 200 and 250 nm is observed, which could correspond to transitions between orbitals located on the ions. This result indicates that the surface of the nanobiohybrids contained an appreciable amount of zinc-organic compound complexes from garlic, as indicated by the results of IR spectroscopy (Figs. 2(b) and (c)), which would contribute appreciably to the UV-Vis spectrum, obscuring the contribution of the ZnO.

3.3 Crystal structure of nanomaterials

In Fig. 3(c), the X-ray diffractogram of the sample synthesized by a chemical route is observed. The peaks of this diffractogram correspond to the wurzite-type ZnO (JCPDS 79-2205) well crystallized. In Fig. 3(d), the X-ray diffractogram of the sample synthesized by a green route is shown. The peaks of this diffractogram correspond to the wurzite type ZnO (JCPDS 79-2205) and the low crystallization of the oxide is evident, possibly due to the presence of garlic in the synthesis system.

Furthermore, this sample was not heat-treated at temperatures higher than 100°C, to obtain ZnO, and only washing the solid precipitate with the water + garlic solution and then drying it favored the formation of the zinc oxide.

Other phases may also be present since peaks could be observed that could not be assigned to a particular compound. This result reiterates the action of the washing process used to obtain the ZnO nanohybrids in the direct conversion of the C-H bonds into desired structures (wurtzite type ZnO), one of the innovative aspects of interest for green chemistry.

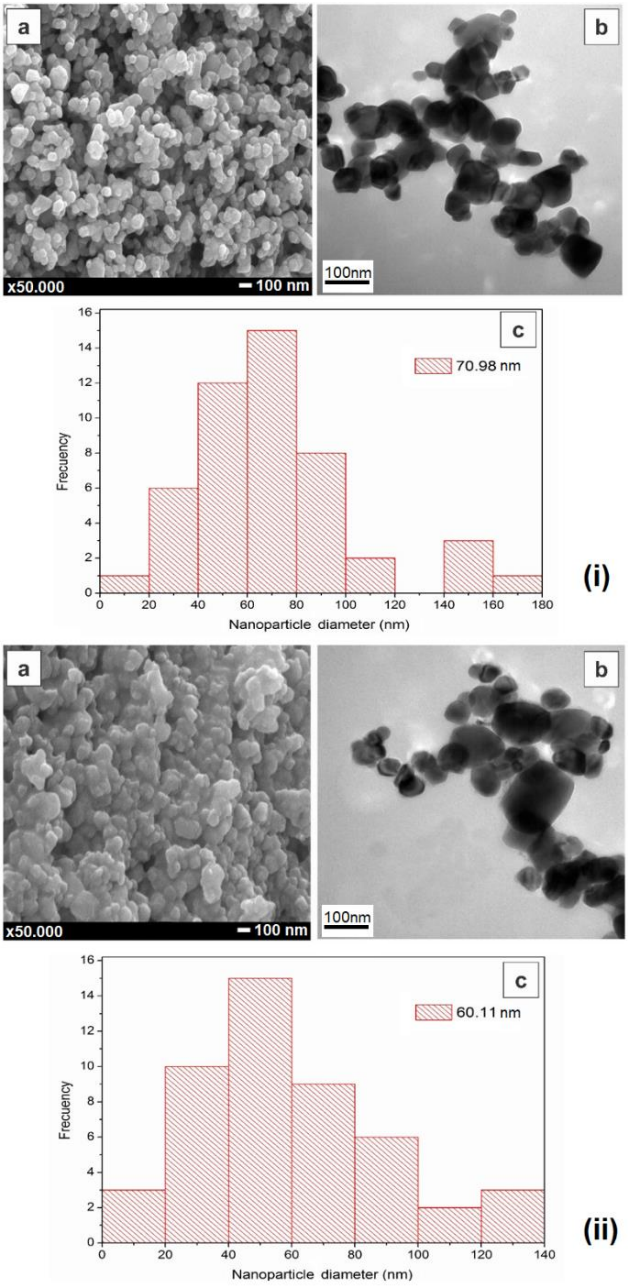

Fig. 4 Micrographs obtained with (a) SEM; (b) TEM, as well as the (c) particle size distribution of the samples of (i) ZnO-NPs synthesized by a chemical route and (ii) nanobiohybrids synthesized by a green route

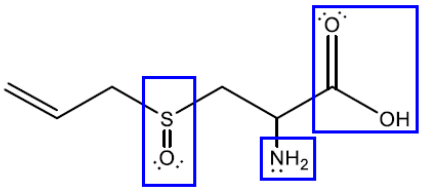

(a) Alliin

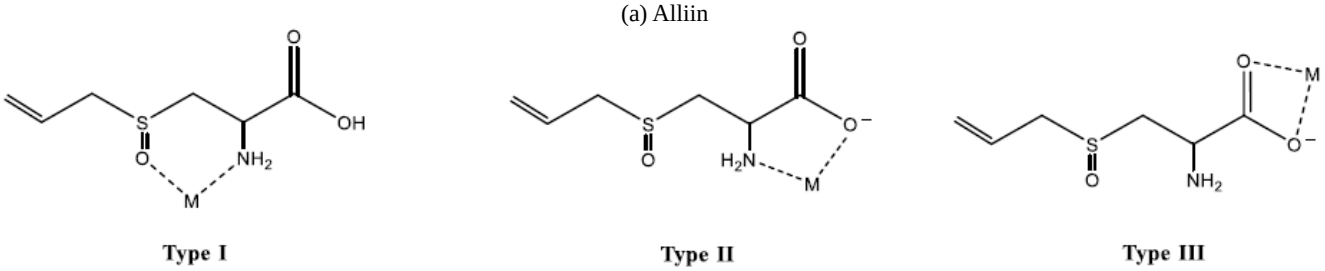

Type I Type II Type III

(b) Possible complexes that Alliin could form with a metal "M"

Scheme 1

3.4 Size and morphology of the synthesized nanomaterials

Fig. 4(i) shows the SEM and TEM micrographs of the ZnO synthesized by chemical route. In these it is observed that the particles had a spheroidal morphology and a particle size smaller than 100 nm (Figs. 4(i-a) and 4(i-b)), quite homogeneous and powders with low agglomeration. In Fig. 4(ii), the micrograph obtained with SEM is observed (Fig. 4(ii-a)) of the nanobiohybrid synthesized by green synthesis. The powder sample presented particles with laminar morphology and a great tendency to stacking which made it difficult to identify the primary particles in the secondary particles (agglomerates). The nanometric characteristics (< 100 nm) and low agglomeration of the nanobiohybrids were evidenced in the micrographs obtained with TEM (Fig. 4(ii-b)).

Considering the results from the characterization of the obtained zinc nanobiohybrids, some reactions that could occur between the complexes that exist in garlic and the zinc ion during the synthesis of these nanomaterials are proposed below, and that could occur during the development of a plausible mechanism to explain their biosynthesis. An analogous proposal, on a biosynthesis mechanism, was previously indicated in the work of Matinise *et al*. (2017) where researchers obtained ZnO-NPs using Moringa olefeira. In the present work, it should be taken into account that the bioactive compounds that exist in garlic mainly contain functional groups such as carboxylic acids, amines, sulfoxides, alkenes and disulfide bonds (Martins *et al*. 2016). Several of these functional groups, rich in electrons, are found in Alliin (Scheme 1(a)), so this compound would be the most likely to act as a binding group during the formation of zinc oxide. In the alliin molecule (Scheme 1(a)) there are three groups that can act as Lewis bases and coordinate with the metal ion (Basolo and Johnson 1967, Demongeot *et al*. 2016), giving rise to three possible metal complexes, such as those indicated in Scheme 1(b).

Specifically, since Zn^{+2} is a class A electron acceptor, it could form more stable complexes with the donor atoms of the second period, oxygen and nitrogen rather than with sulfur (period 3), acting as a strong acid (Ahrland *et al*. 1958). This characteristic and condition of Zn^{+2} would favor the formation of a Type III complex, on reaction of the zinc precursor (zinc acetate dihydrate) with the Alliin, through the reactions indicated in Scheme 2, with the participation of the base that was added to the system as a precipitant.

Deprotonation of the carboxylic acid by the base

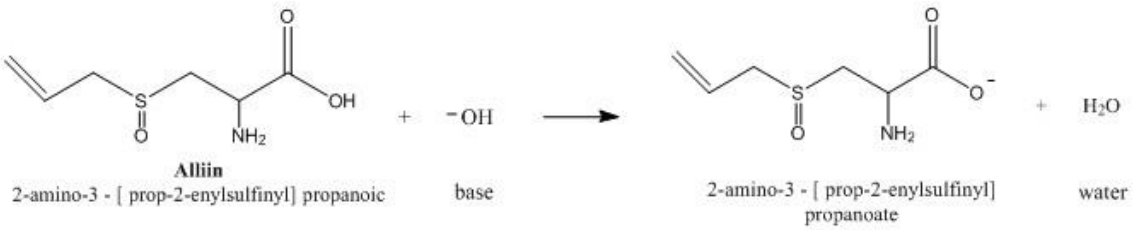

Alliin
2-amino-3 - [prop-2-enylsulfinyl] propanoic

base

2-amino-3 - [prop-2-enylsulfinyl] propanoate

water

In these reactions, the COO^- group would act as a bidentate ligand in the coordination sphere of the zinc (Ahrland *et al*. 1958). In addition, the different stages of washing with the water + garlic solution to which the precipitate obtained was subjected, would guarantee the presence of Alliin in the system, favoring its coordination with zinc and therefore the development of the reactions indicated in Scheme 2.

Meanwhile, the bioactive molecules (E)-ajoene, (Z)-ajoene and Allicin, which are also found in garlic (Martins *et al*. 2016), present sulfoxide groups in their structure in which oxygen, with its free pairs, could coordinate to zinc as indicated in Scheme 3, as with other systems (Glatz *et al*.

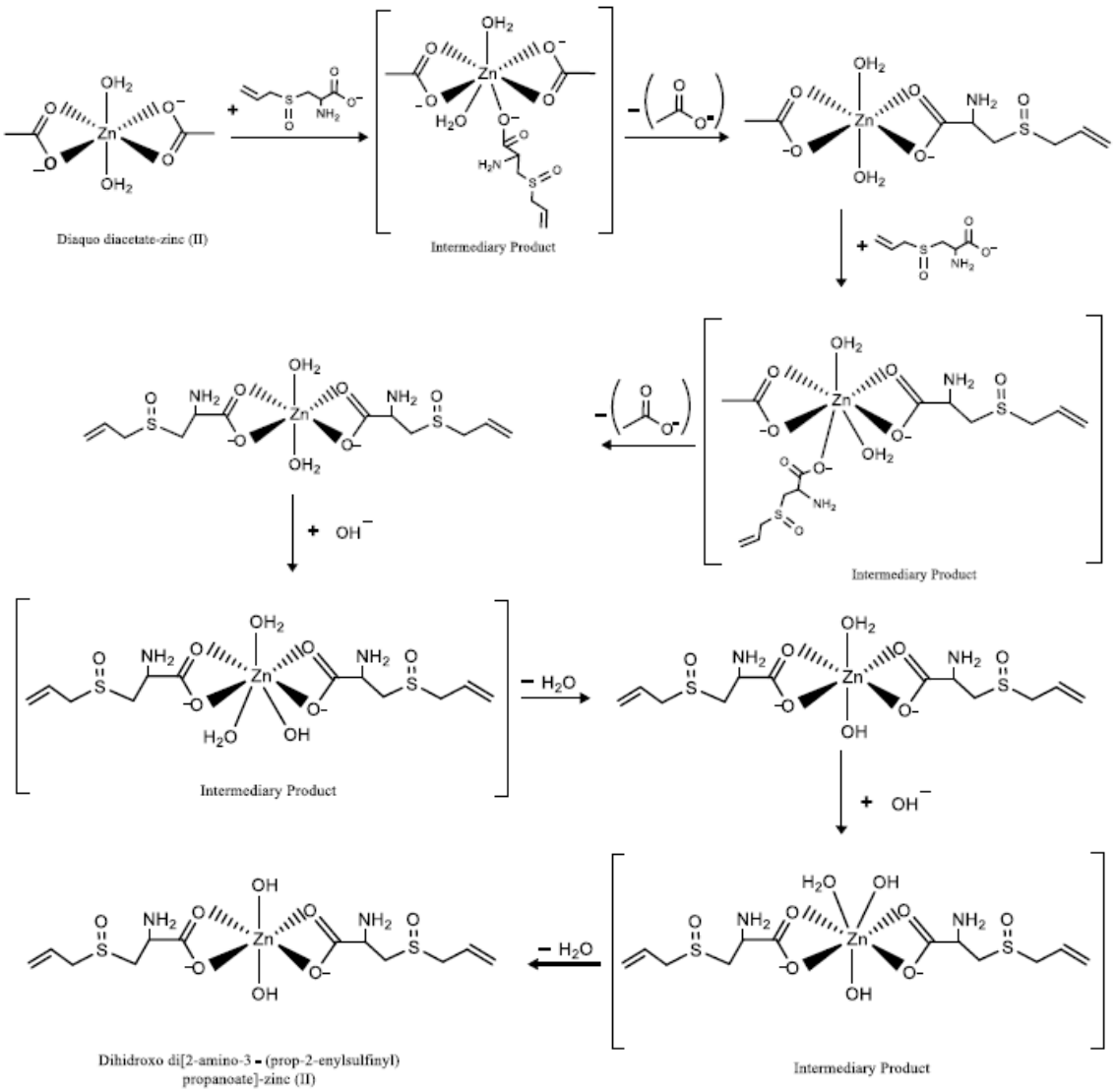

Scheme 2

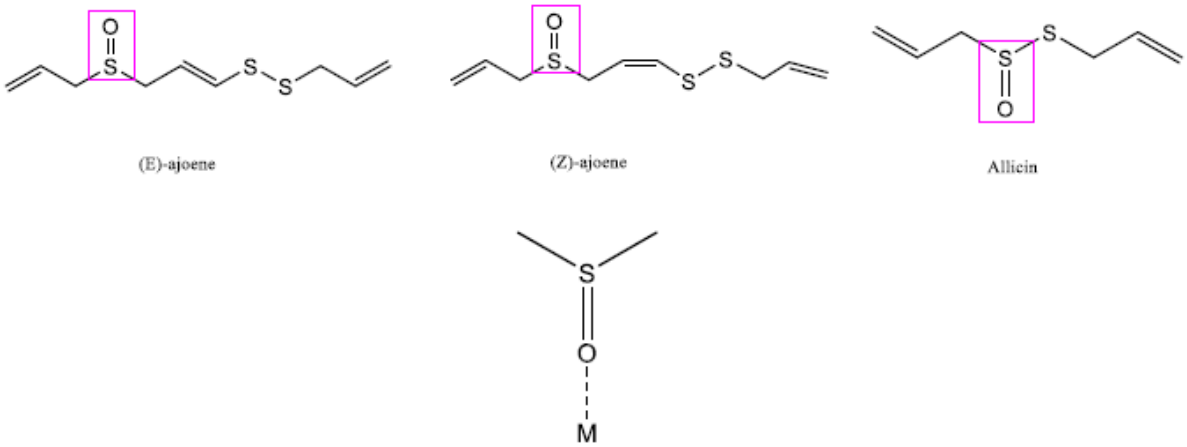

Scheme 3

2016).

The presence, on the surface, of the nanobiohybrid zinc complexes that would form through the reactions indicated in Schemes 2 and 3, would help to explain the results of the characterization with IR (Figs. 2(b) and (c)) and UV-Vis spectroscopies (Fig. 3(b)), as well as with XRD (Fig. 3(d)),

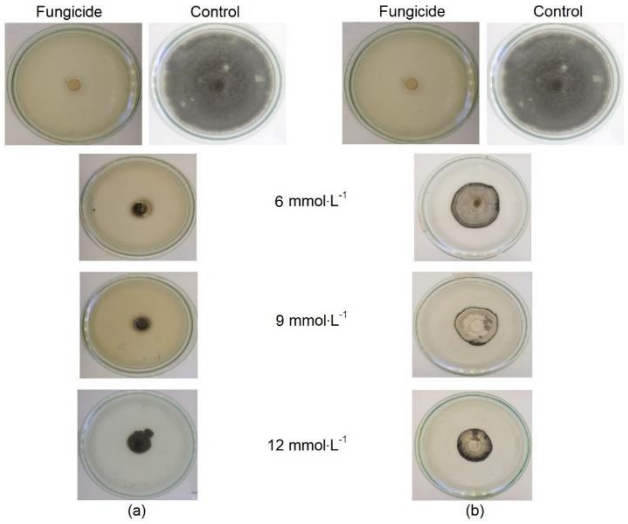

Fig. 5 Macroscopic growth of *Cercospora* sp. after 12 days of testing, considering the antifungal action of the different concentrations of the ZnO-NMs (6, 9 and 12 mmol.L^{-1}), synthesized by: (a) chemical route; (b) green route (nanobio-hybrid). [Control: fungus without treatment; fungicide: fungus treated with commercial Ciproconazole]

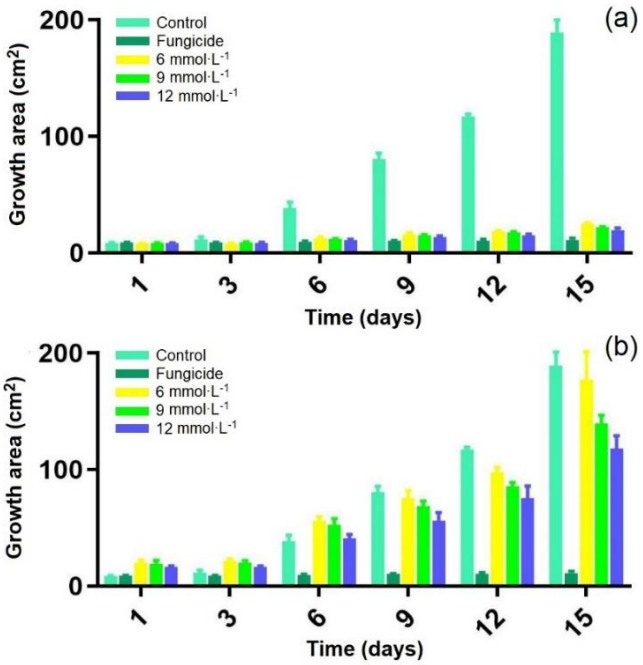

Fig. 6 Bar chart illustrating the growth area of *Cercospora* sp, subjected to the action of: (a) ZnO–NPs (chemical route); (b) nanobio-hybrids (green route) at different concentrations and days [Control: fungus without treatment; fungicide: Fungus treated with commercial Ciproconazole]

of the biosynthesized nanomaterials.

3.5 Action of the synthesized nanofungicides on the coffee crop pathogen isolates

3.5.1 Effect on the Cercospora sp. isolates

3.5.1.1 Macroscopic effect of nanofungicides on the Cercospora sp. isolates

Fig. 5 shows the result of the seeding of *Cercospora* sp. in the bioassays with ZnO-NPs (chemical route) and with ZnO nanobiohybrids (green route), taking as referents the fungicide (PDA culture medium with Ciproconazole - Alto100®) and the control (PDA culture medium without antifungal). At twelve (12) days of observation of the test, the inhibition of the growth of the fungi *Cercospora* sp. through the action of the ZnO-NMs, synthesized by a chemical route (Fig. 5(a)) was more evident than that of those obtained by green route (Fig. 5(b)). For the quantitative analysis of the antifungal capacity of the ZnO-NMs synthesized by a chemical route and the ZnO nanobiohybrids synthesized by green route, the growth area of the fungi subjected to the action of these nanofungicides was measured as a function of time (Fig. 6). In the diagrams of Fig. 6(a) it is observed that the ZnO-NPs, in comparison with the nanobiohybrids (Fig. 6(b)), have a more favorable antifungal activity on the growth of the fungi *Cercospora* sp.; the 12 mmol.L^{-1} concentration being the most efficient (See Table 1).

Table 1 Percentage (%) inhibition of mycelial growth of *Cercospora* sp. with ZnO-NMs synthesized by chemical and green methods

Percent inhibition of mycelial growth								
Pathogen	Control	Fungicide (1:100)*	Treatment					
			12 (mmol.L^{-1})		9 (mmol.L^{-1})		6 (mmol.L^{-1})	
	Cercospora sp.	*Cercospora sp.*	Cr	Gr	Cr	Gr	Cr	Gr
			Cercospora sp.	*Cercospora sp.*	*Cercospora sp.*	*Cercospora sp.*	*Cercospora sp.*	*Cercospora sp.*
Day								
6	0	91.70	70.60	64.62	68.54	55.34	67.17	52.10
9	0	94.44	82.87	69.53	81.26	62.95	79.82	59.08
12	0	96.13	87.10	72.37	85.13	68.96	84.12	64.73

1:1000*: 1 part fungicide to 1000 parts water; Cr: Chemical route; Gr: Green route

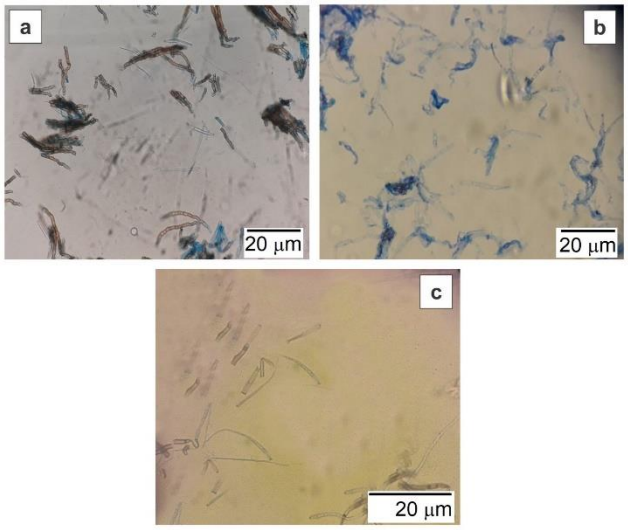

Fig. 7 Images of the reproductive structures (conidiophores and conidia) of *Cercospora* sp. corresponding to samples: (a) control; (b) treated with ZnO-NPs (chemical route - 12 mmol.L^{-1}); (c) treated with ZnO nanobiohybrids (green route - 12 mmol.L^{-1})

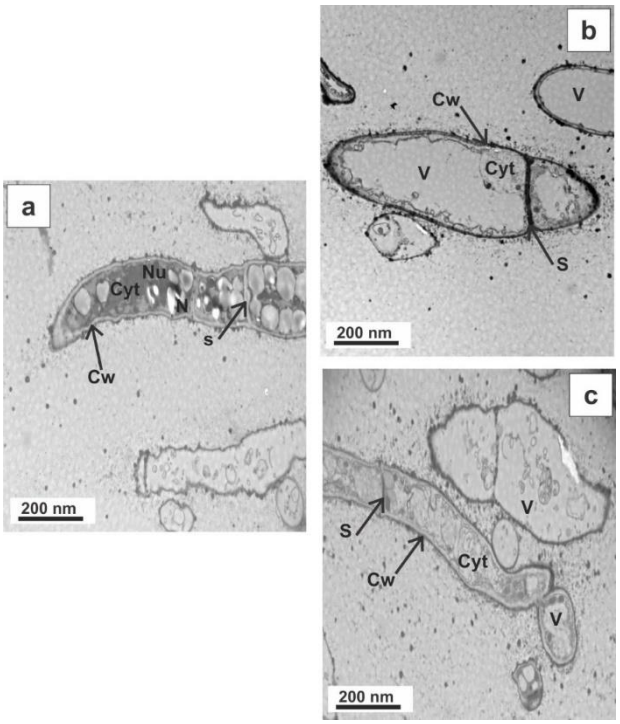

Fig. 8 Micrographs obtained with TEM from *Cercospora* sp.: (a) control and of the fungus subjected to treatment with (b) ZnO-NPs (chemical route); (c) ZnO nanobiohybrids (green route). [Cell wall (Cw), Cytoplasm (Cyt), Nucleus (N), Nucleolus (Nu), Vacuole (V) and Septo (S)]

The data obtained from the percentage of inhibition of the action of the synthesized nanomaterials on *Cercospora* sp, calculated using Eq. (1), are meanwhile indicated in Table 1.

3.5.1.2 Identification of morphological and ultrastructural damages in the Cercospora sp. fungus caused by the treatment with Zno-NPs and nanohybrids

• Morphological changes observed on *Cercospora* sp. with HROM

In Fig. 7(a), we can observe the reproductive structures corresponding to *Cercospora* sp. The dispersed conidia showed an acicular morphology and a hyaline coloration, while the conidiophores showed a yellow to brown coloration, forming units that had several ramifications. Meanwhile, in the sample subjected to treatment with ZnO-NPs obtained by chemical route (12 mmol.L^{-1}: Fig. 7(b)), the presence of conidiophores is not evident, only deformed spots are observed that could be associated with these structures. In addition, the conidia showed a significant change in their morphology, losing their acicular form. On the other hand, in the sample treated with the nanobiohybrids, obtained by green route (12 mmol.L^{-1}: Fig. 7(c)), the development of the reproductive structures occurred normally: the conidia kept their acicular form but underwent a slight elongation and the conidiophores did not present any modification.

• Ultra-structural changes observed on *Cercospora* sp. with TEM

Fig. 8 shows the micrographs obtained with TEM of cells of the *Cercospora* sp. fungus, control (Fig. 8(a)) and subjected to treatments with the synthesized NMs (Figs. 8(b) and (c)). In the ultrafine sections of *Cercospora* sp., corresponding to samples at 12 days of growth, the presence of the characteristic organelles of the cell was observed in the control (Fig. 8(a)). Meanwhile, observing the sample treated with ZnO-NPs obtained by a chemical route (Fig. 8(b)), the displacement of the cytoplasmic content by vacuoles and thinning of the cell wall is imminent. On the other hand, in the sample treated with nanobiohybrids, obtained by a green route, the conservation of cell organelles with an incipient vacuolization process is evident (Fig. 8(c)). These results show a greater aggression, to the ultra-structural part of *Cercospora* sp. by the ZnO-NPs obtained by chemical synthesis.

In general, the results obtained in these tests indicate that the presence of the ZnO-NMs affected the regular growth cycle of *Cercospora* sp., as indicated by the photographs of the growth of the strains (Fig. 5), the growth area bar charts (Fig. 6), the changes in the reproductive structures (Fig. 7), the ultrastructural changes (Fig. 8) and percent inhibition data (Table 1). The strongest inhibition effect was observed with ZnO-NMs obtained by a chemical route.

4. Discussion

Although preliminary ideas exist for structuring a mechanism to explain the action of nanomaterials (NMs) on fungi (Arciniegas-Grijalba *et al*. 2017, 2019, López and Rodríguez-Páez 2017), such as those studied in this work,

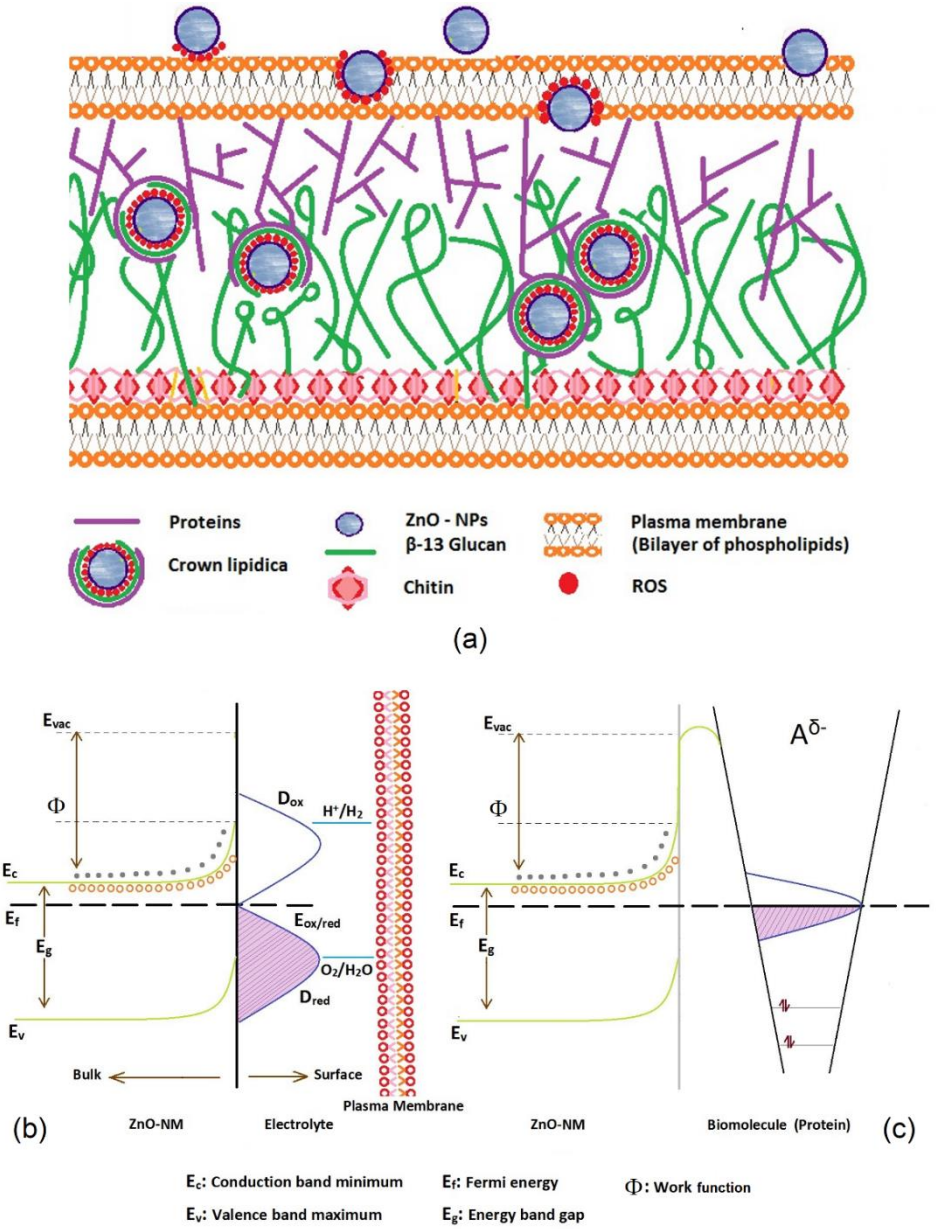

Fig. 9 Diagrams that illustrate: (a) the structure of the cell wall of the fungus and some effects of the interaction of the nanomaterials with the proteins contained in it (adapted from Arciniegas-Grijalba *et al*. (2019)), and the proposed electrical interactions between nanomaterials of ZnO and the (b) cell membrane and (c) biomolecules (proteins)

there is not yet a consolidated and fully verified model. In order to structure the mechanism of action of NMs, it is necessary to identify the main phenomena that occur at the nanomaterial-fungal cell wall surface interface. Fig. 9 shows three diagrams that illustrate the phenomenological model that we propose to qualitatively account for the action of the synthesized ZnO (ZnO-NMs) nanomaterials on the fungi of interest for this work. Undoubtedly, this model requires carrying out, in future, more rigorous systematic investigations using more elaborate experimental techniques.

To explain the results obtained from the inactivation of the fungi *Cercospora* sp., for those in synthesized ZnO-NMs, it is necessary to consider the interaction of these NMs with the biological system, specifically with the cell wall of the fungi. As indicated in Fig. 9(a), the fungal cell wall is composed of glycoproteins and polysaccharides, mainly glucan and chitin (Bowman and Free 2006, Feofilova 2010, Gow *et al*. 2017). Glucan is the most important structural polysaccharide in the fungal cell wall, constituting 50-60% of the wall by dry weight (Kapteyn *et al*. 1999). Chitin on the other hand (long-chain homopolymers of beta-1,4-linked N-acetylglucosamine) is a relatively minor but structurally important component of the fungal cell wall (Bowman and Free 2006, Feofilova 2010, Gow *et al*. 2017). Meanwhile, in the walls of filamentous fungi such as those used in this work, it has been estimated that the amount of proteins present in them can be between 20-30% of the total cell wall mass. Some important proteins in fungi are hydrophobins, amphipathic proteins that can

self-assemble to generate rodlets that produce a hydrophobic interface between filamentous fungi and their environments (Linder 2009).

In general, at the nano-bio (ZnO-NMs-cell wall) interface, dynamic physicochemical interactions as well as kinetic and thermodynamic exchanges ought to occur between the surface of the NMs and the surface of the biological component (e.g., membrane and proteins). This nano-bio interface would consist of three components of dynamic interaction: (1) the surface of the nanomaterial, (2) the solid-liquid interface where the changes in the particle on interacting with the components of the environment occur and (3) the solid-liquid interface in the contact zone with the biological substrate (Nel *et al*. 2009).

Specifically, the most important forces that would act between the NMs, the medium interface and the biological substrate would be long-range ones, attractive van der Waals and repulsive or attractive electrostatic mainly, and short-range forces caused by the existence of charge - steric, depletion and solvent interactions (Min *et al*. 2008). An important interaction of the NMs is with the cellular membrane (Fig. 9(b)) where electrostatic-type forces (Zhang and Yang 2011) and hydrophobic ones are prominent (Hartono *et al*. 2010). These interactions can lead to changes in the two components, both membrane disruption and modification of the surface properties of NMs where the main factors to consider, for analysis and description, would be the concentration of NMs, their composition, size, surface characteristics (Mu *et al*. 2014) and point defects that may be present (Bak *et al*. 2011), among others. Additionally, because the interaction pattern would be supported by the physico-chemical properties of the nano-bio interface, it is expected that the surface potential of the NMs, generated by their surface charge, would induce an electrostatic field around them that could cause re-orientation of the local water molecules (Shapiro and Caspi 2010) as well as of the phospholipids in the membrane (Mu *et al*. 2014). In addition, an interfacial potential can be generated as a result of all the forces of interaction between the NM and the surface of the biomolecules, a potential that would play an important role in the antifungal capacity shown by the ZnO-NMs synthesized in this work, similar to what was evidenced with the antibacterial activity of the ZnO-NPs in the work of Arakha *et al*. (2015). This interfacial potential could lead to the physical rupture of the membrane due to the increase of the surface tension on it, or an increase of Reactive Oxygen Species (ROS), at the interface or within the cell wall of the fungus (Fig. 9(a)).

Elsewhere, recent work by De Lucas-Gil et al. (2013, 2018) puts forward the possibility of mechanisms of an electrical nature involved in the antibacterial and antifungal activity of semiconductors, for example in the ZnO of interest for the present work. These researchers suggest that through the modulation of the orientation of the surface charge of the particles, controlling the morphology of the microstructured ZnO (Ms-ZnO), multiple Schottky-type barriers could be generated that would allow the accumulation of negative charge in localized regions of the structure of Ms-ZnO and that they would act as "charged domain walls". According to the researchers, this charge configuration would improve the microbial activity of the ZnO by an electrical discharging effect because the Ms-ZnO would act as a pulsed electric field propitiating potential discharges against the cell membrane. As a result, these Ms-ZnO would produce a high electric field that would exceed the breakdown potential of the lipid bilayer causing irreparable damage to the membrane (Unal *et al*. 2002).

These results indicate that, in addition to chemical mechanisms (release of Zn^{2+} and ROS cations) (Sirelkhatim *et al*. 2015) and physical ones (abrasion, membrane penetration, direct interaction through electrostatic effects), it is necessary to consider, in greater detail: Entropic mechanisms (Arciniegas-Grijalba *et al*. 2019, Kumar *et al*. 2017) that cause damage to microorganisms; and direct physical interactions (mainly electrical) that take into account the n-type semiconductor nature of ZnO and the electrical behavior of the cell membrane of the fungus (Fig. 9(b)) and of the proteins that make up the corona protein (Figs. 9(a) and (c)). As indicated in Fig. 9(b), in the ZnO-NM-membrane interface it is expected that the conduction bands of the n-type semiconductor ZnO-NMs are curved, favoring the local accumulation of charge carriers, as has been proposed and analyzed for other systems (Bak *et al*. 2011). As indicated previously, one of the components of the nano-bio interface is the solid-liquid interface in the contact zone with the biological substrate (Nel *et al*. 2009), which is illustrated in Fig. 9(b). This interface is metastable in nature because it is subject to an inhomogeneous and dynamic or transient environment due to the distribution and different spatial localization of the structures of proteins, lipids and glycosylated on the cell wall surface membrane. Specifically, the water present in this zone could be adsorbed on the surface of the ZnO-NMs as a result of: (i) A physisorption process in its molecular form and/or (ii) a dissociative chemisorption process. As indicated in Fig. 9(b), the semiconductor/solution interface would acquire an equilibrium condition when the Ox/Red level of the solution, $E°_{ox/red}$, aligns with the Fermi level, EF, of the ZnO (n-type semiconductor) (Gerischer 1990, Nozik and Memming 1996), such that the Fermi energy of the semiconductor would become equal to - $e\mu_e^s$, where μ_e^s is the electrochemical potential of the electron in the solution and "e" the absolute charge of the electron (Lichterman *et al*. 2015). This process would cause a flow of charge between the semiconductor and the solution, generating a region of space charge in the semiconductor, accompanied by an electric field, and therefore the upward band bending in the ZnO, as illustrated in Fig. 9(b). The band bending that would occur in the ZnO-NMs would facilitate the charge separation, repelling the electrons towards the bulk of the semiconductor and attracting the holes towards its surface, causing an enrichment of holes in this place (Zhang and Yates 2012). Charge separation would occur as long as the edge of the conduction band is greater than the hydrogen reduction potential (H^+/H_2) and the edge of the valence band less than the oxidation potential of the water (O_2/H_2O) (Guo *et al*. 2018).

Another important interaction to consider, to account for

the antifungal effect of the ZnO-NMs synthesized in this work, is the one that would occur between the NMs and the proteins that the cell wall of the fungus contains. On the ZnO-NMs entering the physiological environment of the fungus, its surface would be covered by the proteins forming a long-life corona layer ("hard corona"), which is strongly adsorbed to the surface, and a dynamic corona ("soft corona") on top of it (Mahmoudi *et al*. 2016). The adsorption of the proteins on the surface of the ZnO-NMs would be governed by both the affinity of the protein-NM bonds and the protein-protein interactions (Kharazian *et al*. 2016). Specifically, the adsorption of the proteins on the surface of the NMs would be favored by van der Waals type forces, hydrogen bonding and electrostatic and hydrophobic interactions, with the electrostatic type being the most important for the anchoring of proteins to the surface of the NMs: The overall charge of the protein would favor its adsorption. It should be emphasized that the surface of the nanomaterials can induce thermodynamic instabilities on the molecules of the adsorbed proteins. In the work of Saptarshi *et al*. (2013), the most important structural modifications induced by the interaction of NMs with proteins are indicated. From the point of view of biomolecules, the interactions should lead to the formation of coronas of different natures, denaturation of proteins and the formation of NM-protein complexes (Lynch *et al*. 2007, Piella *et al*. 2017), eventually promoting the activation of signaling pathways (Kelly *et al*. 2015) and determining, finally, their physiological response and toxicity (Casals and Puntes 2012).

On entry of the NMs into the cell wall, their interaction with the fungal cell wall could occur through the corona of adsorbed proteins on the nanomaterial surface (Fleischer and Payne 2014, Jayaram *et al*. 2017, Kopp *et al*. 2017). In addition, if the nanofungicides enter the fungal cell wall, they could become trapped, disturbing the intrinsic disorder of the proteins, associated with their structural mobility (Romashchenko *et al*. 2017), as illustrated in Fig. 9(a). The entropic consequences of this disorder-to-order transition would be compensated by their ability to adjust to a structure of the binding partner, in order to wrap or hug the surface of the nanoparticles, resulting in the extensive interaction surface and interaction energy gains. It would also favor the interaction of the proteins with the NMs surface. This action of the nanomaterials could interfere in the synthesis of the proteins, triggering cell responses that would lead to inactivation of the fungus.

Moreover, the electrical interaction between the ZnO-NMs and the proteins (large biomolecules) that are adsorbed on its surface, once the protein corona has formed, can promote electron exchange and therefore the upward band bending in the ZnO, such as is illustrated in Fig. 9(c). As indicated by Zhang et al. in their work (Zhang and Yates 2012), the adsorption of molecules on the surface of a semiconductor can induce band bending close to its surface. Taking into account the adsorption of a biomolecule, for example acceptor (A) on the surface of the ZnO-NM (n-type semiconductor), when it approaches the surface one of its non-full molecular orbitals would interact with the semiconductor and this would shift downward. This interaction would also cause the broadened molecular orbital to accept electrons from the semiconductor, favoring the generation of an electric field and the upward band bending close to the semiconductor surface (Zhang and Yates 2010), as indicated in Fig. 9(c). This band bending effect would affect the transport of charge, holes and electrons, through the ZnO-NM-biomolecule (protein) interface, preventing the passage of electrons to the bulk of the semiconductor and favoring the accumulation of holes in its surface.

Considering the physical interactions of an electrical nature proposed for the ZnO-NM-membrane (Fig. 9(b)) and ZnO-NM-biomolecule (protein) interfaces (Fig. 9(c)), there would be localized electric fields produced by the local accumulation of charge (space charge), which would affect the membrane of the cell wall of the fungus, as proposed by De Lucas-Gil *et al*. (2013, 2018). In addition, it would have its ZnO-NMs surfaces rich in holes that would favor the development of reactions that should lead to the production of ROS, such as the following (Jedsukontorn *et al*. 2018, Nosaka and Nosaka 2017)

$$H_2O + h^+ \rightarrow \bullet OH + H^+ \quad (2)$$

$$2H_2O + 2h^+ \rightarrow H_2O_2 + 2H^+ \quad (3)$$

$$\bullet OH + \bullet OH \rightarrow H_2O_2 \quad (4)$$

generating hydrogen peroxide (H_2O_2) and hydroxyl radicals (•OH) through the oxidation of water present in the nano-bio interface. In addition, considering the existence of hydroxyl groups (OH^-) and the H_2O_2 generated (Eqs. (3) and (4)), the following reactions could also occur (Jedsukontorn *et al*. 2018, Nosaka and Nosaka 2017).

$$H_2O_2 + OH^- \rightarrow HO_2^- + H_2O \quad (5)$$

$$H_2O_2 + 2OH^- + h^+ \rightarrow {}^\bullet O_2^- + 2H_2O \quad (6)$$

with possibility of formation of the radical superoxide, ${}^\bullet O_2^-$, and singlet oxygen, ${}^1O_2$, through the reaction (Min *et al*. 2008)

$${}^\bullet O_2^- + h+ \rightarrow {}^1O_2 \quad (7)$$

Considering the possibility that the reactions indicated in Eqs. (2) to (7) occur, favored by the characteristics of the ZnO-NM-membrane interfaces (Fig. 9(b)) and ZnO-NM-biomolecule (protein) (Fig. 9(c)) generated by the electrical interactions that occur in them, these interfaces would contain an appreciable amount of ROS that would favor an effect of oxidative stress on the fungi, as illustrated in Figs. 7 and 8.

In summary, the ROS generated through the reactions indicated in Eqs. (2) to (7), as well as the localized electric fields generated by the space charge that would exist on the surface of the ZnO-NMs, could cause irreparable damage to the cell membrane of the fungi and therefore the inactivation of the growth of the *Cercospora* sp. fungi, as can be seen in Fig 8. Furthermore, considering the results

obtained in this work where the ZnO-NPs (obtained by a chemical route) and the ZnO nanobiohybrid (synthesized using a "green" route) had a different antifungal effect (Figs. 5 to 8), it is expected that the synthesis method would affect the functionality of the ZnO-NMs obtained, even more so if in the structure of the NMs there are organic molecules (in the present case from the garlic used during the "green" synthesis). The presence of these organic molecules in the bulk and/or on the surface of ZnO ought to affect the phenomena that may occur at the ZnO-NM-membrane interfaces (Fig. 9(b)) as well as at the ZnO-NM-biomolecule (protein) interface (Fig. 9(c)) and therefore the development of the reactions indicated in Eqs. (2) to (7), promoting different antifungal capacity for the ZnO-NMs obtained by a chemical route or using a green route, as evidenced in this work.

In the future, it is necessary to perform a more rigorous study to investigate the variation of the antifungal activity of the NMs by the presence of organic molecules in their structure, as well as to determine experimentally, through specific analytical techniques, the presence of ROS in the ZnO-NM-membrane and ZnO-NM-biomolecule (protein) nano-interfaces and to verify the qualitative phenomenological model proposed in this work, all with the objective of knowing more about the effect of NMs on fungi and on biological systems in general.

Although the antifungal response shown by the zinc nanobiohybrids synthesized in this work is quite promising, it is necessary in future to consider and evaluate in more detail their antioxidant and cytotoxic properties towards normal human cells. As recent studies indicate, biosynthesized nanoxides have different levels of toxicity, depending on the synthesis conditions, which are ultimately what determine their biological characteristics (Stankic *et al*. 2016). For example, work on biosynthesized PbO-NPs carried out by different groups have shown that, for concentrations below 30 μg/mL, they would present an insignificant toxicity (Miri *et al*. 2018), while for other researchers this is not well defined and a more careful study is necessary to evaluate it both *in vitro* and *in vivo* (Khalil *et al*. 2020a). Recent research has evaluated, due to their great technological importance, the toxicity of biosynthesized nanoparticles of nickel oxide (Khalil *et al*. 2017), iron oxide (Sulaiman *et al*. 2018), cerium oxide (Singh *et al*. 2020) and cobalt oxide (Khalil *et al*. 2020b), among others. Specifically, for zinc oxide, its nanoparticles being one of the most toxic (Brunner *et al*. 2006), in the work of Miri *et al*. (2020), both the antifungal activity and cytotoxicity of biosynthesized ZnO-NPS were evaluated using extract of *Proposis farcta* fruit. To do this they used WST-1 assay on MCF7 cell line and the cell viability of the synthesized NPs was observed to be 50.23% in a 500 μg/ml concentration of NPs. Umar *et al*. (2019) studied the biocompatibility and stability of biosynthesized ZnO-NPs and found them to have a high oxidative capacity and cytotoxicity on cancer cell lines. A similar study on murine cell lines was carried out by Namvar *et al*. (2015) and they observed that ZnO-NPs had no effect on normal mouse fibroblasts in treatments for 72 hours.

Therefore, considering the practical application of the nanomaterials, it is necessary to consider their toxic effects. Relevant studies must be carried out that correlate the biosynthesis, stabilization and surface modification of the nanobiohybrids with their biological effects, to decrease their toxicity in light of their practical applications. It is necessary to consider the proposal of Punnoose *et al*. (2014), which indicates that the cytotoxicity of ZnO-NPs can be tailored by modifying their surface bound chemical groups, maintaining the core ZnO structure. This can be achieved through the biosynthesis of ZnO-NPs, obtaining nanobiohybrids, as indicated by the results of this work.

5. Conclusions

Methodologies were structured that allowed us to obtain two different nanofungicides in a controlled and reproducible way: ZnO-NPs by chemical route and nanobiohybrids of ZnO by green route using garlic extract as solvent. Considering the structural and optical characterization of the samples, the one that presented the greatest variation in its properties was that synthesized by green route. In this sample, complete crystallization of ZnO was not observed. There were modifications in both the IR and UV-Vis spectra in addition to presenting agglomerates of laminar particles and not spheroidal particles as observed in the sample obtained by precipitation (chemical pathway). Furthermore, considering the results of the effect of the nanofungicides synthesized on the coffee crop fungal pathogen *Cercospora* sp., it was found that the treatment with ZnO-NPs (chemical route) caused the highest percent inhibition for *Cercospora* sp. (~87.1%).

The morphological and ultra-ultrastructural effects of the nanofungicides on the fungi studied became evident in the HROM and TEM studies. These studies showed appreciable vacuolization and thinning of the cell wall, as well as liquefaction of the cytoplasmic content in the cells of the fungi, *Cercospora* sp., when treated with ZnO-NPs (chemical route) and ZnO nanobiohybrids (green route). Under the conditions of the experiments tested in this paper, it is shown that the efficiency of the nanofungicides would be correlated with the technique of obtaining them: chemical synthesis or green synthesis. Additionally, based on bibliographic information and the results of IR spectroscopy obtained in this work, a nanoscale mechanism of ZnO biosynthesis from zinc acetate dihydrate was proposed. The reaction of the zinc precursor with different bioactive compounds of garlic ((E)-ajoene, (Z)-ajoene and Allicin) was proposed, mainly with Alliin.

Acknowledgments

We are grateful to COLCIENCIAS for funding relating to project code number 110365842673 COLCIENCIAS ID 4241 and to the VRI for providing logistical support. We are especially grateful to Colin McLachlan for suggestions relating to the English text.

References

Aala, F., Yusuf, U.K., Nulit, R. and Rezaie, S. (2014), "Inhibitory effect of allicin and garlic extracts on growth of cultured hyphae", *Iran. J. Basic Med. Sci.*, **17**, 150.

Abd-Elsalam, K.A. and Alghuthaymi, M.A. (2015), "Nanobio-fungicides: Are they the next-generation of fungicides", *J. Nanotech. Mater. Sci.*, **2**, 1-3. https://doi.org/10.15436/2377-1372.15.0.

Agarwal, H., Venkat Kumar, S. and Rajeshkumar, S. (2017), "A review on green synthesis of zinc oxide nanoparticles – an eco-friendly approach", *Resour. Technol.*, **3**, 406-413. https://doi.org/10.1016/j.reffit.2017.03.002.

Ahmed, S., Annu Chaudhry, S.A. and Ikram, S. (2017), "A review on biogenic synthesis of ZnO nanoparticles using plant extracts and microbes: A prospect towards green chemistry", *J. Photochem. Photobiol. B Biol.*, **166**, 272-284. https://doi.org/10.1016/j.jphotobiol.2016.12.011.

Ahrland, S., Chatt, J. and Davies N.R. (1958), "The relative affinities of ligand atoms for acceptor molecules and ions", *Q. Rev. Chem. Soc.*, **12**, 265-276. https://doi.org/10.1039/QR9581200265.

Aladpoosh, R. and Montazer, M. (2015), "The role of cellulosic chains of cotton in biosynthesis of ZnO nanorods producing multifunctional properties: Mechanism, characterizations and features", *Carbohydr. Polym.*, **126**, 122-129. https://doi.org/10.1016/j.carbpol.2015.03.036.

Ali, K., Dwivedi, S., Azam, A., Saquib, Q., Al-Said, M.S., Alkhedhairy, A.A. and Musarrat, J. (2016), "Aloe vera extract functionalized zinc oxide nanoparticles as nanoantibiotics against multi-drug resistant clinical bacterial isolates", *J. Colloid Interface Sci.*, **472**, 145-156. https://doi.org/doi.org/10.1016/j.jcis.2016.03.021.

Alwan, R.M., Kadhim, Q.A., Sahan, K.M., Ali, R.A., Mahdi, R.J., Kassim, N.A. and Jassim, A.N. (2015), "Synthesis of zinc oxide nanoparticles via sol-gel route and their characterization", *Nanosci. Nanotechnol.*, **5**, 1-6. https://doi.org/10.5923/j.nn.20150501.01.

Ambika, S. and Sundrarajan, M. (2015), "Antibacterial behaviour of Vitex negundo extract assisted ZnO nanoparticles against pathogenic bacteria", *J. Photochem. Photobiol. B Biol.*, **146**, 52-57. https://doi.org/10.1016/j.jphotobiol.2015.02.020.

Anbuvannan, M., Ramesh, M., Viruthagiri, G., Shanmugam, N. and Kannadasan, N. (2015), "Anisochilus carnosus leaf extract mediated synthesis of zinc oxide nanoparticles for antibacterial and photocatalytic activities", *Mater. Sci. Semicond. Process*, **39**, 621-628. https://doi.org/10.1016/j.mssp.2015.06.005.

Arakha, M., Saleem, M., Mallick, B.C. and Jha, S. (2015), "The effects of interfacial potential on antimicrobial propensity of ZnO nanoparticle", *Sci. Rep.*, **5**, 9578. https://doi.org/10.1038/srep09578.

Arciniegas-Grijalba, P.A., Patiño-Portela, M.C., Mosquera-Sánchez, L.P., Guerrero-Vargas, J.A. and Rodríguez-Páez, J.E. (2017), "ZnO nanoparticles (ZnO-NPs) and their antifungal activity against coffee fungus Erythricium salmonicolor", *Appl. Nanosci.*, **7**, 225-241. https://doi.org/10.1007/s13204-017-0561-3.

Arciniegas-Grijalba, P.A., Patiño-Portela, M.C., Mosquera-Sánchez, L.P., Guerra Sierra, B.E., Muñoz-Florez, J.E., Erazo-Castillo, L.A. and Rodríguez-Páez, J.E. (2019), "ZnO-based nanofungicides: Synthesis, characterization and their effect on the coffee fungi Mycena citricolor and Colletotrichum sp", *Mater. Sci. Eng. C*, **98**, 808-825. https://doi.org/10.1016/j.msec.2019.01.031.

Arndtsen, B.A., Bergman, R.G., Mobley, T.A. and Peterson, T.H. (1995), "Selective intermolecular carbon-hydrogen bond activation by synthetic metal complexes in homogeneous solution", *Acc. Chem. Res.*, **28**, 154-162. https://doi.org/10.1021/ar00051a009.

Avila, H., Cruz, M., Villegas, M., Caballero, C. and Rodríguez-Páez, J.E. (2004), "Estudio comparativo de dos metodos de sintesis para la obtencion de polvos cerámicos de ZnO-Pr[Comparative study of two methods of synthesis to obtain ceramic powders of ZnO - Pr]", *Bol. Soc. Esp. Ceram.*, **43**, 740-744 (in Spanish).

Bak, T., Nowotny, J., Sucher, N.J. and Wachsman, E. (2011), "Effect of crystal imperfections on reactivity and photoreactivity of TiO_2 (Rutile) with oxygen, water and bacteria", *J. Phys. Chem. C*, **115**, 15711-15738. https://doi.org/10.1021/jp2027862.

Basolo, F. and Johnson, R.C. (1967), "Química de los compuestos de coordinación[Coordination Chemistry]", Editorial Reverte, Barcelona, España (in Spanish).

Beckman, E.J. (2003), "Oxidation reactions in CO_2: Academic exercise or future green processes?", *Environ. Sci. Technol.*, **37**, 5289-5296. https://doi.org/10.1021/es034540i.

Bowman, S.M. and Free, S.J. (2006), "The structure and synthesis of the fungal cell wall", *Bioessays*, **28**(8), 799-808. https://doi.org/10.1002/bies.20441.

Bozzola, J.J. and Russell, L.D. (1999), *Electron Microscopy: Principles and Techniques for Biologists*, Jones and Bartlett, Toronto, Canada.

Brunner, T.J., Wick, P., Manser, P., Spohn, P., Grass, R.N., Limbach, L.K., Bruinink, A. and Stark, W.J. (2006), "*In vitro* cytotoxicity of oxide nanoparticles: Comparison to asbestos, silica, and the effect of particle solubility", *Environ. Sci. Technol.*, **40**, 4374-4381. https://doi.org/10.1021/es052069i.

Buzea, C., Pacheco, I.I. and Robbie, K. (2007), "Nanomaterials and nanoparticles: Sources and toxicity". *Biointerphases*, **2**, 17-71. https://doi.org/10.1116/1.2815690.

Casals, E. and Puntes, V.F. (2012), "Inorganic nanoparticle biomolecular corona: Formation, evolution and biological impact", *Nanomedicine*, **7**(12), 1917-1930. https://doi.org/10.2217/nnm.12.169.

Crabtree, R.H. (2004), "Organometallic alkane CH activation", *J. Organomet. Chem.*, **689**, 4083-4091. https://doi.org/10.1016/j.jorganchem.2004.07.034.

Cui, X., Yin, J., Lin, Y., Li, N., Wang, M. and Shen, D., (2016), "Towards a definition of harmless nanoparticles from an environmental and safety perspective", *J. Chem.*, **2016**, 1-12. https://doi.org/10.1155/2016/8608567.

Dakhlaoui, A., Jendoubi, M., Smiri, L.S., Kanaev, A. and Jouini, N. (2009), "Synthesis, characterization and optical properties of ZnO nanoparticles with controlled size and morphology", *J. Cryst. Growth*, **311**, 3989-3996. https://doi.org/10.1016/j.jcrysgro.2009.06.028.

De Lucas-Gil, E., Reinosa, J.J., Neuhaus, K., Vera-Londono, L., Martín-González, M., Fernández, J.F. and Rubio-Marcos, F. (2017), "Exploring new mechanisms for effective antimicrobial materials: Electric contact-killing based on multiple Schottky barriers", *ACS Appl. Mater. Interfaces*, **9**(31), 26219-26225. https://doi.org/10.1021/acsami.7b09695.

De Lucas-Gil, E., Leret, P., Monte-Serrano, M., Reinosa, J.J., Enríquez, E., Del Campo, A., Cañete, M., Menéndez, J., Fernández, J.F. and Rubio-Marcos, F. (2018), "ZnO nanoporous spheres with broad-spectrum antimicrobial activity by physicochemical interactions", *ACS Appl. Nano Mater.*, **1**, 3214-3225. https://doi.org/10.1021/acsanm.8b00402.

Demongeot, A., Mougnier, S.J., Okada, S., Soulie-Ziakovic, C. and Tournilhac, F. (2016), "Coordination and catalysis of Zn^{2+} in epoxy-based vitrimers", *Polym. Chem.*, **7**, 4486-4493. https://doi.org/10.1039/C6PY00752J.

Djurišić, A.B. and Leung, Y.H. (2006), "Optical properties of ZnO nanostructures", *Small*, **2**, 944-961. https://doi.org///doi.org/10.1002/smll.200600134.

Dobrucka, R. and Długaszewska, J. (2016), "Biosynthesis and antibacterial activity of ZnO nanoparticles using Trifolium pratense flower extract", *Saudi. J. Biol. Sci.*, **23**, 517-523. https://doi.org///doi.org/10.1016/j.sjbs.2015.05.016.

Feofilova, E.P. (2010), "The fungal cell wall: Modern concepts of its composition and biological function", *Microbiology*, **79**, 711-720. https://doi.org/10.1134/S0026261710060019.

Fiévet, F. and Brayner, R. (2013), *Nanomaterials: A Danger or a Promise?*, Springer, London, UK. https://doi.org/10.1007/978-1-4471-4213-3.

Fleischer, C.C. and Payne, C.K. (2014), "Nanoparticle-cell interactions: Molecular structure of the protein corona and cellular outcomes", *Acc. Chem. Res.*, **47**, 2651-2659. https://doi.org/10.1021/ar500190q.

Gerischer, H. (1990), "The impact of semiconductors on the concepts of electrochemistry", *Electrochim. Acta*, **35**(11-12), 1677-1699. https://doi.org/10.1016/0013-4686(90)87067-C.

Glatz, M., Schroffenegger M., Weil, M. and Karl Kirchner, K. (2016), "Crystal structure of hexakis (dimethyl sulfoxide-κO) manganese(II) diiodide", *Acta Cryst.*, **72**, 904-906. http://dx.doi.org/10.1107/S2056989016008896.

Gow, N.A.R., Latge, J.P. and Munro, C.A. (2017), *The Fugal Kingdom*, ASM Press, Washington, USA. https://doi.org/10.1128/microbiolspec.FUNK-0035-2016.

Guo, J. and Peng, C. (2015), "Synthesis of ZnO nanoparticles with a novel combustion method and their C_2H_5OH gas sensing properties", *Ceram. Int.*, **41**, 2180-2186. https://doi.org/10.1016/j.ceramint.2014.10.017.

Guo, Z., Ambrosio, F., Chen, W., Gono, P. and Pasquarello, A. (2018), "Alignment of redox levels at semiconductor-water interfaces", *Chem. Mater.*, **30**, 94-111. https://doi.org/10.1021/acs.chemmater.7b02619.

Hartono, D., Hody Yang, K.L. and Lanry Yung, L.Y. (2010), "The effect of cholesterol on protein-coated gold nanoparticle binding to liquid crystal-supported models of cell membranes", *Biomaterials*, **31**, 3008-3015. https://doi.org/10.1016/j.biomaterials.2010.01.003.

He, L., Liu, Y., Mustapha, A. and Lin, M. (2011), "Antifungal activity of zinc oxide nanoparticles against Botrytis cinerea and Penicillium expansum", *Microbiol. Res.*, **166**, 207-215. https://doi.org/10.1016/j.micres.2010.03.003.

Heiligtag, F.J. and Niederberger, M. (2013), "The fascinating world of nanoparticle research", *Mater. Today*, **16**, 262-271. https://doi.org/10.1016/j.mattod.2013.07.004.

Hussain, I., Singh, N.B., Singh, A., Singh, H. and Singh, S.C. (2016), "Green synthesis of nanoparticles and its potential application", *Biotechnol. Lett.*, **38**, 545-560. https://doi.org/10.1007/s10529-015-2026-7.

Jafarirad, S., Mehrabi, M., Divband, B. and Kosari-Nasab, M. (2016), "Biofabrication of zinc oxide nanoparticles using fruit extract of Rosa canina and their toxic potential against bacteria: A mechanistic approach", *Mater. Sci. Eng. C*, **59**, 296-302. https://doi.org/10.1016/j.msec.2015.09.089.

Jagadish, C. and Pearton, S.J. (2006), *Zinc Oxide Bulk, Thin Films and Nanostructures: Processing, Properties, and Applications*, Elsevier, Amsterdam, Netherlands.

Janotti, A. and Van de Walle, C.G. (2009), "Fundamentals of zinc oxide as a semiconductor", *Rep. Prog. Phys.*, **72**, 126501. https://doi.org/10.1088/0034-4885/72/12/126501.

Jayaram, D.T., Runa, S., Kemp, M.L. and Payne, C.K. (2017), "Nanoparticle-induced oxidation of corona proteins initiates an oxidative stress response in cells", *Nanoscale*, **9**, 7595-7601. https://doi.org/10.1039/C6NR09500C.

Jedsukontorn, T., Ueno, T., Saito, N. and Hunsom, M. (2018), "Mechanistic aspect based on the role of reactive oxidizing species (ROS) in macroscopic level on the glycerol photooxidation over defected and defected-free TiO_2", *J. Photochem. Photobiol. A Chem.*, **367**, 270-281. https://doi.org/10.1016/j.jphotochem.2018.08.030.

Kairyte, K., Kadys, A. and Luksiene, Z. (2013), "Antibacterial and antifungal activity of photoactivated ZnO nanoparticles in suspension", *J. Photochem. Photobiol. B Biol.*, **128**, 78-84. https://doi.org/10.1016/j.jphotobiol.2013.07.017.

Kapteyn, J.C., Van Den Ende, H. and Klis, F.M. (1999), "The contribution of cell wall proteins to the organization of the yeast cell wall", *Biochim. Biophys. Acta Gen. Subj.*, **1426**, 373-383. https://doi.org/10.1016/S0304-4165(98)00137-8.

Kelly, P.M., Åberg, C., Polo, E., O'Connell, A., Cookman, J., Fallon, J., Krpetić, Ž. and Dawson, K.A. (2015), "Mapping protein binding sites on the biomolecular corona of nanoparticles", *Nat. Nanotechnol.*, **10**, 472-479. https://doi.org/10.1038/nnano.2015.47.

Khalil, A.T., Ovais, M., Ullah, I., Ali, M., Shinwari, Z.K., Hassan, D. and Maaza, M. (2017), "Sageretia thea (Osbeck) modulated biosynthesis of NiO nanoparticles and their in vitro pharmacognostic, antioxidant and cytotoxic potential", *Artif. Cells Nanomed. Biotechnol.*, **46**(4), 838-852. https://doi.org/10.1080/21691401.2017.1345928.

Khalil, A.T., Ovais, M., Ullah, I., Ali, M., Jan, S.A., Shinwari, Z.K. and Maaza, M. (2020a), "Bioinspired synthesis of pure massicot phase lead oxide nanoparticles and assessment of their biocompatibility, cytotoxicity and *in-vitro* biological properties", *Arab. J. Chem.*, **13**, 916-931. http://dx.doi.org/10.1016/j.arabjc.2017.08.009.

Khalil, A.T., Ovais, M., Ullah, I., Ali, M., Shinwari, Z.K. and Maaza, M. (2020b), "Physical properties, biological applications and biocompatibility studies on biosynthesized single-phase cobalt oxide (Co_3O_4) nanoparticles via Sageretia thea (Osbeck)", *Arab. J. Chem.*, **13**, 606-619. http://dx.doi.org/10.1016/j.arabjc.2017.07.004.

Khan, I., Saeed, K. and Khan, I. (2017), "Nanoparticles: Properties, applications and toxicities", *Arab. J. Chem.*, **12**(7), 908-931. https://doi.org/10.1016/j.arabjc.2017.05.011.

Kharazian, B., Hadipour, N.L. an Ejtehadi, M.R., (2016), "Understanding the nanoparticle-protein corona complexes using computational and experimental methods", *Int. J. Biochem. Cell Biol.*,**75**, 162-174. https://doi.org/10.1016/j.biocel.2016.02.008.

Kharissova, O.V., Dias, H.V.R., Kharisov, B.I., Pérez, B.O. and Pérez, V.M.J. (2013), "The greener synthesis of nanoparticles", *Trends Biotechnol.*, **31**, 240-248. https://doi.org/10.1016/j.tibtech.2013.01.003.

Kisch, H. (2014), *Semiconductor Photocatalysis: Principles and Applications*, Wiley, Weinheim, Germany.

Klingshirn, C. (2007), "ZnO: From basics towards applications", *Phys. Status Solidi*, **244**, 3027-3073. https://doi.org/10.1002/pssb.200743072.

Klingshirn, C.F., Waag, A., Hoffmann, A. and Geurts, J. (2010), *Zinc Oxide: From Fundamental Properties towards Novel Applications*, Springer Science and Business Media, Berlin, Germany.

Kołodziejczak-Radzimska, A. and Jesionowski, T. (2014), "Zinc oxide-from synthesis to application: A review", *Materials*, **7**, 2833-2881. https://doi.org/10.3390/ma7042833.

Kopp, M., Kollenda, S. and Epple, M. (2017), "Nanoparticle-protein interactions: Therapeutic approaches and supramolecular chemistry", *Acc. Chem. Res.*, **50**, 1383-1390. https://doi.org/10.1021/acs.accounts.7b00051.

Krupa, A. and Vimala, R. (2016), "Evaluation of tetraethoxysilane (TEOS) sol-gel coatings, modified with green synthesized zinc oxide nanoparticles for combating microfouling", *Mater. Sci. Eng. C*, **61**, 728-735. https://doi.org/10.1016/j.msec.2016.01.013

Kumar, A. and Kumar, J. (2008a), "Defect and adsorbate induced

infrared modes in sol-gel derived magnesium oxide nano-crystallites", *Solid State Commun*., **147**, 405-408. https://doi.org/10.1016/j.ssc.2008.06.014.

Kumar, A. and Kumar, J. (2008b), "On the synthesis and optical absorption studies of nano-size magnesium oxide powder", *J. Phys. Chem. Solids*, **69**, 2764-2772. https://doi.org/10.1016/j.jpcs.2008.06.143.

Kumar, R., Umar, A., Kumar, G. and Nalwa, H.S. (2017), "Antimicrobial properties of ZnO nanomaterials: A review", *Ceram. Int*., **43**, 3940-3961. https://doi.org/10.1016/j.ceramint.2016.12.062.

Lead, J.R. and Smith, E.L. (2009), *Environmental and Human Health Impacts of Nanotechnology*, John Wiley & Sons, Chichester, UK. https://doi.org/10.1002/9781444307504.

Lear, T., Marshall, R., Antonio Lopez-Sanchez, J., Jackson, S.D., Klapötke, T.M., Bäumer, M., Rupprechter, G., Freund, H.J. and Lennon, D. (2005), "The application of infrared spectroscopy to probe the surface morphology of alumina-supported palladium catalysts", *J. Chem. Phys*., **123**, 174706. https://doi.org///doi.org/10.1063/1.2101487.

Ledezma, E. and Apitz-Castro, R. (2006), "Ajoene, el principal compuesto activo derivado del ajo (Allium sativum), un nuevo agente antifúngico", *Rev. Iberoam. Micol*., **23**, 75-80. https://doi.org/10.1016/S1130-1406(06)70017-1.

Li, C.J. (2016), "Reflection and perspective on green chemistry development for chemical synthesis-Daoist insights", *Green Chem*., **18**, 1836-1838. https://doi.org/10.1039/C6GC90029A.

Li, C.J. and Trost, B.M. (2008), "Green chemistry for chemical synthesis", *Proc. Natl. Acad. Sci*., **105**, 13197-13202. https://doi.org/10.1073/pnas.0804348105.

Li, J., Sang, H., Guo, H., Popko, J.T., He, L., White, J.C., Parkash Dhankher, O., Jung, G. and Xing, B. (2017), "Antifungal mechanisms of ZnO and Ag nanoparticles to Sclerotinia homoeocarpa", *Nanotechnology*, **28**, 155101. https://doi.org/10.1088/1361-6528/aa61f3.

Lichterman, M.F., Hu, S., Richter, M.H., Crumlin, E.J., Axnanda, S., Favaro, M., Drisdell, W., Hussain, Z., Mayer, T., Brunschwig, B.S., Lewis, N.S., Liu, Z. and Lewerenz, H.J. (2015), "Direct observation of the energetics at a semiconductor/liquid junction by operando X-ray photoelectron spectroscopy", *Energy Environ. Sci*., **8**, 2409-2416. https://doi.org/10.1039/C5EE01014D.

Linder, M.B. (2009), "Hydrophobins: Proteins that self assemble at interfaces", *Curr. Opin. Colloid Interface Sci*., **14**, 356-363. https://doi.org/10.1016/j.cocis.2009.04.001.

López, C. and Rodríguez-Páez, J.E. (2017), "Synthesis and characterization of ZnO nanoparticles: Effect of solvent and antifungal capacity of NPs obtained in ethylene glycol.", *Appl. Phys. A*, **123**, 748-764. https://doi.org/10.1007/s00339-017-1339-x.

Lynch, I., Cedervall, T., Lundqvist, M., Cabaleiro-Lago, C., Linse, S. and Dawson, K.A. (2007), "The nanoparticle-protein complex as a biological entity; a complex fluids and surface science challenge for the 21st century", *Adv. Colloid Interface Sci*., **134-135**, 167-174. https://doi.org/10.1016/j.cis.2007.04.021.

Mahmoudi, M., Bertrand, N., Zope, H. and Farokhzad, O.C. (2016), "Emerging understanding of the protein corona at the nano-bio interfaces", *Nano Today*, **11**, 817-832. https://doi.org/10.1016/j.nantod.2016.10.005.

Martins, N., Petropoulos, S. and Ferreira, I.C.F.R. (2016), "Chemical composition and bioactive compounds of garlic (Allium sativum L) as affected by pre- and post-harvest conditions: A review", *Food Chem.*, **211**, 41-50. http://dx.doi.org/10.1016/j.foodchem.2016.05.029.

Matinise, N., Fuku, X.G., Kaviyarasu, K., Mayedwa, N. and Maaza, M. (2017), "ZnO nanoparticles via Moringa oleifera green synthesis: Physical properties and mechanism of formation", *Appl. Surf. Sci*., **406**, 339-347. http://dx.doi.org/10.1016/j.apsusc.2017.01.219.

Min, Y., Akbulut, M., Kristiansen, K., Golan, Y. and Israelachvili, J. (2008), "The role of interparticle and external forces in nanoparticle assembly", *Nat. Mater*., **7**, 527-538. https://doi.org/10.1038/nmat2206.

Miri, A., Sarani, M., Hashemzadeh, A., Mardani, Z. and Darroudi, M. (2018), "Biosynthesis and cytotoxic activity of lead oxide nanoparticles", *Green Chem. Lett. Rev*., **11**(4), 567-572. https://doi.org/10.1080/17518253.2018.1547926.

Miri, A., Khatami, M., Ebrahimy, O. and Sarani, M. (2020), "Cytotoxic and antifungal studies of biosynthesized zinc oxide nanoparticles using extract of Prosopis farcta fruit", *Green Chem. Lett. Rev*., **13**(1), 27-33. https://doi.org/10.1080/17518253.2020.1717005.

Mitchnick, M.A., Fairhurst, D. and Pinnell, S.R. (1999), "Microfine zinc oxide (Z-cote) as a photostable UVA/UVB sunblock agent", *J. Am. Acad. Dermatol*., **40**, 85-90. https://doi.org///doi.org/10.1016/S0190-9622(99)70532-3.

Moharram, A.H., Mansour, S.A., Hussein, M.A. and Rashad, M. (2014), "Direct precipitation and characterization of ZnO nanoparticles", *J. Nanomater*., **2014**, 1-5. https://doi.org/10.1155/2014/716210.

Morkoç, H. and Özgür, Ü. (2008), *Zinc Oxide: Fundamentals, Materials and Device Technology*, Wiley, Weinheim, Germany.

Motulsky, H. (2007), "In GraphPad prism 5: Statistics Guide, GraphPad software inc", Press San Diego, California, USA.

Mu, Q., Jiang, G., Chen, L., Zhou, H., Fourches, D., Tropsha, A. and Yan, B. (2014), "Chemical basis of interactions between engineered nanoparticles and biological systems", *Chem. Rev*., **114**, 7740-7781. https://doi.org/10.1021/cr400295a.

Muhsin, T.M., Al-Zubaidy, S.R. and Ali, E.T. (2001), "Effect of garlic bulb extract on the growth and enzymatic activities of rhizosphere and rhizoplane fungi", *Mycopathologia*, **152**, 143-146. https://doi.org/10.1023/A:1013184613159.

Namvar, F., Rahman, H.S., Mohamad, R., Susan Azizi, S., Tahir, P.M., Chartrand, M.S. and Yeap, S.K. (2015), "Cytotoxic effects of biosynthesized zinc oxide nanoparticles on murine cell lines", *Evid. Based Complementary Altern. Med*., **2015**, 593014. http://dx.doi.org/10.1155/2015/593014.

Narayan, S., Muldoon, J., Finn, M.G., Fokin, V.V, Kolb, H.C. and Sharpless, K.B. (2005), "Cover picture: 'on water': Unique reactivity of organic compounds in aqueous suspension (Angew. Chem. Int. ed. 21/2005)", *Angew. Chem. Int. Ed*., **44**, 3157-3157. https://doi.org/10.1002/anie.200590069.

Nealon, G.L., Donnio, B., Greget, R., Kappler, J.P., Terazzi, E. and Gallani, J.L. (2012), "ChemInform abstract: Magnetism in gold nanoparticles", *ChemInform*, **43**, 44. https://doi.org/10.1002/chin.201244226.

Nel, A., Xia, T., Madler, L. and Li, N. (2006), "Toxic potential of materials at the nanolevel", *Science*, **311**, 622-627. https://doi.org/10.1126/science.1114397.

Nel, A.E., Mädler, L., Velegol, D., Xia, T., Hoek, E.M.V., Somasundaran, P., Klaessig, F., Castranova, V. and Thompson, M. (2009), "Understanding biophysicochemical interactions at the nano-bio interface", *Nat. Mater*., **8**, 543-557. https://doi.org/10.1038/nmat2442.

Nosaka, Y. and Nosaka, A.Y. (2017), "Generation and detection of reactive oxygen species in photocatalysis", *Chem. Rev*., **117**, 11302-11336. https://doi.org/10.1021/acs.chemrev.7b00161.

Nozik, A.J. and Memming, R. (1996), "Physical chemistry of semiconductor-liquid interfaces", *J. Phys. Chem*., **100**, 13061-13078. https://doi.org/10.1021/jp953720e.

Parveen, K., Banse, V. and Ledwani, L. (2016), "Green synthesis of nanoparticles: Their advantages and disadvantages", *AIP Conf. Proc*., **1724**, 020048. https://doi.org/10.1063/1.4945168.

Piella, J., Bastús, N.G. and Puntes, V. (2017), "Size-dependent protein-nanoparticle interactions in citrate-stabilized gold nanoparticles: The emergence of the protein corona", *Bioconjug. Chem.*, **28**, 88-97. https://doi.org/10.1021/acs.bioconjchem.6b00575.

Prasad, R. (2016), *Advances and Applications Through Fungal Nanobiotechnology, Fungal Biology*, Springer International Publishing, Switzerland. https://doi.org/10.1007/978-3-319-42990-8.

Punnoose, A., Dodge, K., Rasmussen, J., Chess, J., Wingett, D. and Anders, C. (2014), "Cytotoxicity of ZnO nanoparticles can be tailored by modifying their surface structure: A green chemistry approach for safer nanomaterials", *ACS Sustain. Chem. Eng.*, **2**(7), 1666-1673. http://dx.doi.org/10.1021/sc500140x.

Qian, Y., Yao, J., Russel, M., Chen, K. and Wang, X. (2015), "Characterization of green synthesized nano-formulation (ZnO-A. vera) and their antibacterial activity against pathogens", *Environ. Toxicol. Pharmacol.*, **39**, 736-746. https://doi.org/10.1016/j.etap.2015.01.015.

Ray, P.C., Yu, H. and Fu, P.P. (2009), "Toxicity and environmental risks of nanomaterials: Challenges and future needs", *J. Environ. Sci. Health C Environ. Carcinog. Ecotoxicol. Rev.*, **27**, 1-35. https://doi.org/10.1080/10590500802708267.

Rideout, D.C. and Breslow, R. (1980), "Hydrophobic acceleration of Diels-Alder reactions", *J. Am. Chem. Soc.*, **102**, 7816-7817. https://doi.org/10.1021/ja00546a048.

Rodríguez-Paéz, J., Caballero, A., Villegas, M., Moure, C., Durán, P. and Fernández, J. (2001), "Controlled precipitation methods: Formation mechanism of ZnO nanoparticles", *J. Eur. Ceram. Soc.*, **21**, 925-930. https://doi.org/10.1016/S0955-2219(00)00283-1.

Romashchenko, A.V., Kan, T.W., Petrovski, D.V., Gerlinskaya, L.A., Moshkin, M.P. and Moshkin, Y.M. (2017), "Nanoparticles associate with intrinsically disordered RNA-binding proteins", *ACS Nano*, **11**, 1328-1339. https://doi.org/10.1021/acsnano.6b05992.

Romero de Pérez, G. (2003), "Microscopía electrónica de transmisión (MET) área biomédica: teoría y práctica [Electron microscopy of transmission (TEM) biomedical area: theory and practice]", *Acad. Colomb. Defic. exactas físicas y Nat. Colección Julio Carrizosa Val*, **12**, 207 (in Spanish).

Saptarshi, S.R., Duschl, A. and Lopata, A.L. (2013), "Interaction of nanoparticles with proteins: Relation to bio-reactivity of the nanoparticle", *J. Nanobiotechnol.*, **11**, 26. https://doi.org/10.1186/1477-3155-11-26.

Shapiro, S. and Caspi, E. (1998), "The steric course of enzymic hydroxylation at primary carbon atoms", *Tetrahedron*, **54**, 5005-5040. https://doi.org/10.1002/chin.199831320.

Shapiro, S. and Caspi, E. (2010), "ChemInform abstract: The steric course of enzymic hydroxylation at primary carbon atoms", *ChemInform*, **29**, 5005-5040. https://doi.org/10.1002/chin.199831320.

Sharma, D., Rajput, J., Kaith, B.S., Kaur, M. and Sharma, S. (2010), "Synthesis of ZnO nanoparticles and study of their antibacterial and antifungal properties", *Thin Solid Films*, **519**, 1224-1229. https://doi.org/10.1016/j.tsf.2010.08.073.

Sheldon, R.A. (2005), "Green solvents for sustainable organic synthesis: State of the art", *Green Chem.*, **7**, 267. https://doi.org/10.1039/b418069k.

Singh, K.R.B., Nayak, V., Tanushri Sarkar, T. and Singh R.P. (2020), "Cerium oxide nanoparticles: Properties, biosynthesis and biomedical application", *RSC Adv.*, **10**, 27194-27214. https://doi.org/10.1039/d0ra04736h.

Sirelkhatim, A., Mahmud, S., Seeni, A., Kaus, N.H.M., Ann, L.C., Bakhori, S.K.M., Hasan, H. and Mohamad, D. (2015), "Review on zinc oxide nanoparticles: Antibacterial activity and toxicity mechanism", *Nano-Micro Lett.*, **7**, 219-242. https://doi.org/10.1007/s40820-015-0040-x.

Stankic, S., Sternig, A., Finocchi, F., Bernardi, J., Diwald, O., (2010), "Zinc oxide scaffolds on MgO nanocubes", *Nanotechnology*, **21**, 355603. https://doi.org/10.1088/0957-4484/21/35/355603.

Stankic, S., Suman, S., Haque, F. and Vidic, J. (2016), "Pure and multi metal oxide nanoparticles: Synthesis, antibacterial and cytotoxic properties", *J. Nanobiotechnol.*, **14**, 73. https://doi.org/ 10.1186/s12951-016-0225-6.

Sulaiman, G.M., Tawfeeq, A.T. and Naji, A.S. (2018), "Biosynthesis, characterization of magnetic iron oxide nanoparticles and evaluations of the cytotoxicity and DNA damage of human breast carcinoma cell lines", *Artif. Cells, Nanomed. Biotechnol.*, **46**(6), 1215-1229. https://doi.org/10.1080/21691401.2017.1366335.

Tansey, M.R. and Appleton, J.A. (1975), "Inhibition of fungal growth by garlic extract", *Mycologia*, **67**, 409-413.

Timonin, M.I. and Thexton, R.H. (1951), "The rhizosphere effect of onion and garlic on soil microflora1", *Soil Sci. Soc. Am. J.*, **15**, 186. https://doi.org/10.2136/sssaj1951.036159950015000C0042x.

Tripathi, D.K., Ahmad, P., Sharma, S., Chauhan, D.K. and Dubey, N.K. (2017), *Nanomaterials in Plants, Algae, and Microorganisms: Concepts and Controversies*, Elsevier, London, UK.

Trost, B.M. (1991), "The atom economy-a search for synthetic efficiency", *Science*, **254**, 1471-1477. https://doi.org/10.1126/science.1962206.

Umar, H., Kavaz, D. and Rizaner, N. (2019), "Biosynthesis of zinc oxide nanoparticles using Albizia lebbeck stem bark, and evaluation of its antimicrobial, antioxidant, and cytotoxic activities on human breast cancer cell lines", *Int. J. Nanomed.*, **14**, 87-100. https://doi.org/10.2147/IJN.S186888.

Unal, R., Yousef, A.E. and Dunne, C.P. (2002), "Spectrofluorimetric assessment of bacterial cell membrane damage by pulsed electric field", *Innov. Food Sci. Emerg. Technol.*, **3**, 247-254. https://doi.org/10.1016/S1466-8564(02)00033-4.

Virkutyte, J. and Varma, R.S. (2013), *Sustainable Nanotechnology and the Environment: Advances and Achievements*, ACS Publications, Washington. USA. https://doi.org/10.1021/bk-2013-1124.ch002.

Woll, C. (2007), "The chemistry and physics of zinc oxide surfaces", *Prog. Surf. Sci.*, **82**, 55-120. https://doi.org/10.1016/j.progsurf.2006.12.002.

Xing, B., Vecitis, C.D. and Senesi, N. (2016), *Engineered Nanoparticles and the Environment: Biophysicochemical Processes and Toxicity*, John Wiley & Sons, Hoboken, USA. https://doi.org/10.1002/9781119275855.

Yang, L., Wang, J. and Xiang, L. (2015), "Hydrothermal synthesis of ZnO whiskers from ε-$Zn(OH)_2$ in $NaOH/Na_2SO_4$ solution", *Particuology*, **19**, 113-117. https://doi.org/10.1016/j.partic.2014.06.010.

Yoshida, S., Kasuga, S., Hayashi, N., Ushiroguchi, T., Matsuura, H. and Nakagawa, S. (1987), "Antifungal activity of ajoene derived from garlic", *Appl. Environ. Microbiol.*, **53**, 615-617.

Zar, J.H. (2014), *Bioestatistical Analysis*, Pearson Education Limited, Harlow, UK.

Zhang, Z. and Yates, J.T. (2010), "Effect of adsorbed donor and acceptor molecules on electron stimulated desorption: O_2 /TiO_2(110)", *J. Phys. Chem. Lett.*, **1**, 2185-2188. https://doi.org/10.1021/jz1007559.

Zhang, X. and Yang, S. (2011), "Nonspecific adsorption of charged quantum dots on supported zwitterionic lipid bilayers: Real-time monitoring by quartz crystal microbalance with dissipation", *Langmuir*, **27**, 2528-2535.

https://doi.org/10.1021/la104449y.
Zhang, Z. and Yates, J.T. (2012), “Band bending in semiconductors: Chemical and physical consequences at surfaces and interfaces”, *Chem*. *Rev*., **112**, 5520-5551. https://doi.org/10.1021/cr3000626.

JL